Characterization of hevin (SPARCL1) immunoreactivity in postmortem human brain homogenates

Amaia Nuñez-Delmoral, Iria Brocos-Mosquera, Vincent Vialou, Luis F Callado, Amaia M Erdozain

Characterization of hevin (SPARCL1) immunoreactivity in *postmortem* human brain homogenates.

Amaia Nuñez-delMoral[1,2], Iria Brocos-Mosquera[1,2], Vincent Vialou[3,4,5], Luis F. Callado[1,2,6], Amaia M. Erdozain[1,2]

[1] Department of Pharmacology, University of the Basque Country, UPV/EHU, Leioa, Bizkaia, Spain
[2] Centro de Investigación Biomédica en Red de Salud Mental (CIBERSAM), Spain
[3] Sorbonne Université, Neuroscience Paris Seine – IBPS, Team Neurobiology of Psychiatric Disorders, Paris, France.
[4] CNRS UMR8246, Neuroscience Paris Seine - IBPS, Team Neurobiology of Psychiatric Disorders, Paris, France.
[5] Inserm U1130, Neuroscience Paris Seine – IBPS, Team Neurobiology of Psychiatric Disorders, Paris, France.
[6]BioCruces Bizkaia Health Research Institute, Barakaldo, Bizkaia, Spain

Corresponding authors: Amaia M. Erdozain and Vincent Vialou
Department of Pharmacology, University of the Basque Country (UPV/EHU), Barrio Sarriena s/n, 48940 Leioa, Bizkaia, Spain. Tel: +34-946012762 | Fax:+34-946013220. ORCID ID: 0000-0003-0207-9122. Email address: amaia_erdozain@ehu.eus
Sorbonne Université, INSERM, CNRS, Neuroscience Paris Seine, 75005, Paris, France. Tel : +33-144276098 | Fax:+33-144276069. ORCID ID: 0000-0002-8212-751X. Email address: vincent.vialou@inserm.fr

Keywords: hevin, SPARCL1, human brain, *postmortem*, western blot

ABSTRACT

Hevin is a matricellular glycoprotein that plays important roles in neural developmental processes such as neuronal migration, synaptogenesis and synaptic plasticity. In contrast to other matricellular proteins whose expression decreases when development is complete, hevin remains highly expressed, suggesting its involvement in adult brain function. *In vitro* studies have shown that hevin can have different post-translational modifications. However, the glycosylation pattern of hevin in the human brain remains unknown, as well as its relative distribution and localization. The present study provides the first thorough characterization of hevin protein expression by western blot in *postmortem* adult human brain. Our results demonstrated two major specific immunoreactive bands for hevin: an intense band migrating around 130 kDa, and a band migrating around 100 kDa. Biochemical assays revealed that both hevin bands have a different glycosylation pattern. Subcellular fractionation showed greater expression in membrane-enriched fraction than in cytosolic preparation, and a higher expression in prefrontal cortex compared to hippocampus, caudate nucleus and cerebellum. We confirmed that ADAMTS4 and MMP-3 proteases digestion led to an intense double band with similar molecular weight to that described as SPARC-like fragment. Finally, hevin immunoreactivity was also detected in human astrocytoma, meningioma, cerebrospinal fluid and serum samples, but was absent from any blood cell type.

INTRODUCTION

Hevin, also called SPARC-like1 (SPARCL1 or SC1), ECM2 or Mast9, is a matricellular glycoprotein of the secreted protein acidic and rich in cysteine (SPARC) family (Girard & Springer, 1996; Johnston et al., 1990; Soderling et al., 1997). Non-structural matricellular proteins (including hevin, SPARC, thrombospondin and tenascin families) are extracellular matrix (ECM) molecules that do not act directly as scaffold molecules, but interact with other ECM proteins as well as cytokines, proteases, neurotrophic factors and cell surface receptors (Bornstein, 1995). As a consequence of their cell-cell and cell-ECM interactions during brain development, these proteins take part in cell proliferation, differentiation, neuronal migration and synaptogenesis (Bornstein, 2009; Bornstein & Sage, 2002; Eroglu, 2009; Murphy-Ullrich & Sage, 2014). Hevin distribution along radial glial fibers in the developing cortex signals the end of neuronal migration in the appropriate cortical layer due to its antiadhesive properties (Gongidi et al., 2004). During synaptogenesis, hevin expression in astrocytes promotes the formation of excitatory synapses during brain development (Kucukdereli et al., 2011; Risher et al., 2014), probably by bridging non-interacting presynaptic neurexin-1α and postsynaptic neuroligin-1B proteins (Singh et al., 2016).

Whereas most of the matricellular proteins are expressed mostly during brain development, hevin remains highly expressed in adult brain (Eroglu, 2009; Lively et al., 2007; Lloyd-Burton & Roskams, 2012; Weaver et al., 2011). Recently, we identified hevin cellular expression profile in adult human brain, specifically in astrocytes and in various types of neurons, in particular in GABAergic parvalbumin-positive neurons, as well as other GABAergic neuronal subtypes and some glutamatergic neurons (Mongrédien et al., 2019). The systematic comparison between mouse and human adult brain revealed a conserved cellular expression pattern for hevin (Mongrédien et al., 2019; Weaver et al., 2011). Hevin is found in all mouse brain regions by virtue of its astrocytic expression and has been observed in every human brain region studied so far including prefrontal cortex, caudate nucleus, brainstem and sensory ganglion neurons (Hashimoto et al., 2016; Mongrédien et al., 2019). Its physiological role in adult brain has been investigated mainly in animal models of brain diseases such as brain injury, ischemic infarction and epilepsy. Thus, hevin expression is enhanced in reactive astrocytes after ischemic infarction or localized brain injury in adult rodents (Lively et al., 2011; McKinnon & Margolskee, 1996; Mendis et al., 2000). In a study of behavioral adaptation to stress, hevin was induced in resilient individuals and its overexpression

by viral-mediated transgenesis reversed the effects of social defeat in mice acting like an antidepressant (Vialou et al., 2010). Accordingly, hevin is one of the most downregulated transcripts in the frontopolar cortex of depressed/suicide victims (Zhurov et al., 2012). Hevin has also been looked at as a potential biomarker of neurodegenerative disorders and has been found in the cerebrospinal fluid (CSF) of individuals with Parkinson´s and Alzheimer´s diseases (Yin et al., 2009).

Post-translational modifications are essential to the physiological function of extracellular proteins (Correia et al., 2019). Hevin is a 80 kDa protein that is post-translationally modified, mainly by glycosylation. The glycosylation pattern of hevin was first described in rat brain in 1990 (Johnston et al., 1990); it was thereafter studied in recombinant hevin in an eukaryotic expression system (Hambrock et al., 2003), and described in human CSF (Halim et al., 2013; Nilsson et al., 2009). However, so far no study has assessed hevin's glycosylation pattern in human brain tissue. In addition, despite being characterized as a synaptic junction protein in rodents (Kucukdereli et al., 2011; Risher et al., 2014; Singh et al., 2016), the subcellular distribution of the protein hevin in human brain remains unknown. In the present study, we provide the first detailed characterization of hevin immunoreactivity by western blot in several *postmortem* human brain regions. First, we performed the biochemical characterization of hevin proteolysis, deglycosylation and protease cleavage pattern. Second, we performed regional and subcellular expression analyses of hevin in human prefrontal cortex (PFC), hippocampus (HIP), cerebellum (CB) and caudate nucleus (CAU). Sex and age-differences in hevin immunoreactivities in human PFC were also analyzed. In addition, we explored the expression levels of hevin protein in human astrocytomas, meningiomas, CSF and blood samples.

EXPERIMENTAL PROCEDURES

Materials

The different primary antibodies used in this study (catalogue number, type, dilutions) are detailed in Table 1. Goat-IgG anti-mouse biotin (B 2763) was obtained from ThermoFisher Scientific. Recombinant human hevin (2728-SL) and recombinant human ADAMTS4 (A Disintegrin and Metalloproteinase with Thrombospondin motifs 4, 4307-AD) proteins were obtained from R&D Systems. Thrombin, was purchased from Sigma-Aldrich (605195) and human MMP-3 protein (Matrixmetalloproteinase 3, 10467-HNAE) from Sino Biological. EndoF3 (Endoglycosidase F3, P0771S), EndoH (Endoglycosidase H, P0702S) and PNGaseF (N-Glycosidse F, P0708S) recombinant enzymes were obtained from New England BioLabs.

Human samples

Human samples from subjects who died by sudden and violent causes were obtained at autopsy in the Basque Institute of Legal Medicine, Bilbao, Spain. All the subjects died by sudden and violent causes; *postmortem* tissue examinations and medical histories determined they were free of psychiatric or neurological disorders. At the time of autopsy, samples from the brain PFC, CAU, HIP, CB and CSF were extracted, at the time of autopsy and immediately stored at −70°C until assayed. Small pieces of brain tissue containing tumor were collected at the time of craniotomy for tumor resection at the Neurosurgery Service, Cruces Hospital (Bizkaia, Spain) and stored at –70°C until assays were performed. Samples were also taken from each patient for diagnosis by neuropathologists according to the International Classification of CNS (central nervous system) tumors drafted under the auspices of the World Health Organization. The tumors were diagnosed as anaplastic astrocytoma (grade III) or meningioma. Samples of blood were immediately processed after extraction from living subjects. The demographic characteristics and the number of the subjects included in the different types of experiments are shown in

Table 2. The study was performed in compliance with legal policy and ethical review boards for *postmortem* brain studies.

Hevin knock out mouse brain samples

Hevin-null mice were obtained from C. Eroglu (Duke University, North Carolina, USA). Hevin-null mice were generated using homologous recombination of the second exon at the transcription start codon resulting in the absence of hevin protein expression (McKinnon et al., 2000). Hevin-null mice were backcrossed to C57BL/6J for 10 generations. Experiments were performed on brains of 2 to 4 months old hevin-null, wild-type (WT) littermates and C57BL/6J mice, after sacrifice. Briefly, mice were decapitated and their brain quickly removed. Cerebellum was dissected and stored at -80°C. Samples were homogenized by sonication in 200 µl of RIPA buffer 1X containing protease inhibitor at 1/1000 on ice (Sigma, Protease Inhibitor Cocktail #11836153001). Protein concentrations were determined by Bradford assay (Bradford, 1976). Proteins samples (50 µg) were suspended in NuPage LDS sample buffer 25% (Invitrogen, Carlsbad, CA, USA, #NP0008) and DTT 1M, heated at 90°C for 10 min, and then analyzed by western blot. All experiments were performed in conformity with the European Union laws and policies for use of animals in neuroscience research (European Committee Council Directive 2010/63/EU), and were approved by the local animal research committee. C57BL6J mice were housed in groups under conditions at 22±1°C and a 12 h light/dark cycle, with food and water provided ad libitum.

Hevin expressing cells

Human carcinoid BON cells maintained in 1:1 DMEM/F12 supplemented with 10% fetal bovine serum and 100 U-100 µg/ml of penicillin-streptomycin, at 37°C in a humidified 5% CO_2 incubator, were transiently transfected with mHevin or mock-transfected, using Lipofectamine 2000 standard protocol. Cells were lysed in 5 mM Tris-HCl Tris-HCl pH 7.4 with a sonicator and then analysed by western blot.

Preparation of brain subcellular fractions

Human brain samples were prepared in order to obtain total homogenates, cytosolic/soluble fractions and membrane-enriched (P2) fraction, as previously described (Brocos-Mosquera et al., 2018), with minor modifications.

Preparation of CSF samples and blood fractionation

Human *postmortem* CSF samples were centrifuged for 10 min (4°C) at 1100xg to remove cell and debris, as previously published (Collins et al., 2015). For blood fractionation (n=4), 5 mL of blood were added slowly to a 5 mL density bar (0.9 mL OptiprepTM, 0.85% (w/v) NaCl, 20 nM Hepes-NaOH pH 7.4, 1 mM EDTA) to avoid mixing the two phases, and centrifuged 15 min (20°C) at 350×g on a swinging rotor (Eppendorf centrifuge 5810 R, A-4-62 rotor). Whole blood was separated into four phases that were recovered separately, corresponding to serum (top phase), platelets (intermediate thin layer), leucocytes (intermediate layer, under platelets) and erythrocytes (bottom phase) enriched fractions. To remove any serum content of fractions enriched in platelets and leucocytes, they were centrifuged again (5 min, 20°C 600×g) and the supernatants were discharged. The pellet was resuspended in 500 µL of resuspending solution (0.85% (w/v) NaCl, 20 nM Hepes-NaOH pH 7.4, 1 mM EDTA) and centrifuged again. Homogenization buffer supplemented with protease and phosphatase inhibitors was added to each blood fraction and sonicated for 15 s (QSONICA Q55). Protein content was measured by the Bradford method (Collins et al., 2015) and stored at -70°C until analyzed by western blot.

Western blot

Western blot assays were performed as previously described (Brocos-Mosquera et al., 2018) with the exception of degradation assays and specificity assays, in which the primary antibody was incubated (1 h at room temperature) with the blocking peptide (R&D Systems 2728-SL, 1:150) in the same incubation solution prior to incubation with the nitrocellulose membrane. The hevin immunoreactivity values were normalized to β-actin signal. A standard pool of total homogenate was processed on the same gels and used as external reference sample.

Immunoprecipitation assay

Immunoprecipitation assays were performed as previously described (Brocos-Mosquera et al., 2018). Polyclonal goat anti-hSPARCL1 antibody (R&D Systems AF2728) was used for immunoprecipitations and goat IgG were used as isotype control of unspecific binding. Lysates were precleared 1 h at 4°C with protein A/G agarose (Santa Cruz, sc-2003) and incubated with 10 μg antibody for 100 μg of tissue and protein A/G agarose beads at 4°C overnight. After three washes with lysis buffer, samples were heated at 95°C for 7 min in loading buffer for elution and centrifuged to pellet the agarose beads. Western blot was used to analyze the supernatants.

Protein identification by LC-MS/MS

Selected bands were excised manually from the gel and subjected to in-gel endopeptidase digestion as previously published (Shevchenko et al., 1996), with minor modifications. Gel pieces were incubated with DTT (10 mM in 50 mM NH_4HCO_3, 56^{o}C, 45 min) and Iodoacetamide (25 mM in 50 mM NH_4HCO_3, room temperature, 30 min, dark) and digested with proteomics grade trypsin (12.5 ng/μl in 50mM NH_4HCO_3, 37^{o}C, overnight). The recovered peptides were dried in a SpeedVac (Thermo Fisher Scientific) and desalted with homemade C18 tips (3M Empore C18). Mass spectrometric analyses were performed on an EASY-nLC 1200 liquid chromatography system interfaced with a Q Exactive HF-X mass spectrometer (Thermo Scientific) via a nanospray flex ion source. Desalted peptides were loaded onto an Acclaim PepMap100 precolumn (75 μm x 2 cm, Thermo Scientific) connected to an Acclaim PepMap RSLC (75 μm x 25 cm, Thermo Scientific) analytical column. Peptides were eluted using a linear gradient of 2.4 to 24% acetonitrile in 0.1% formic acid at a flow rate of 300 nL min^{-1} over 18 min. Full MS scans were acquired from m/z 375 to 1800 with a resolution of 120,000 at m/z 200. The 10 most intense ions were fragmented by higher energy C-trap dissociation with normalized collision energy of 28 and MS/MS spectra were recorded with a resolution of 15,000 at m/z 200. The maximum ion injection time was 100 ms for survey and 120 ms for MS/MS scans, whereas AGC target values of 3 x 10^6 and 5 x 10^5 were used for survey and MS/MS scans, respectively(Elu et al., 2019). Raw files were processed with Proteome Discoverer 2.2 (Thermo Scientific) and searches were performed against a UniProtKB-SwissProt Human (2020_02) database. Precursor and fragment mass tolerances were set to 10 ppm and 0.02 Da respectively and up to 1 missed cleavage was allowed. Carbamidomethylation of Cys was set as fixed modification and oxidation of Met as variable modification. Peptide and protein FDR were set to 1%.

Deglycosylation assays

Following the manufacturers recommendations, 8 μg of total homogenates obtained from a pool of human PFC or 50 ng of human recombinant hevin (R&D Systems, 2728-SL) as positive control were treated with three deglycosylases separately: EndoF3 (50 U), EndoH (5000 U) and PNGase F (1000 U). Briefly, samples were incubated in the appropriate reaction buffer (final volume of 20 μl), in the presence or absence of the enzyme, for 5 h at 37°C. The reaction was stopped by addition of a final concentration

of PMSF 2 mM, DTT 100 mM, Laemmli buffer (2% SDS, 8% glycerol, 0.01% bromophenol blue), and by heating for 5 min at 98°C, before being analyzed by western blot.

Proteolysis study

A pool of total homogenates obtained from human PFC was prepared in the presence or absence of protease inhibitors, as previously published (Brocos-Mosquera et al., 2018), and incubated at 37°C for a range of time (0–180 min). Then samples were prepared in the loading buffer, heated at 95°C for 5 min and analyzed by western blot. In temperature-dependent proteolysis assays, a range of different temperatures (4°C–95°C, for 15 min) was used to heat the samples in the loading buffer.

ADAMTS4, MMP-3 and Thrombin proteases digestion

140 µg of total protein of PFC pool were combined with 2 µg of ADAMTS4 or 0.4 µg of MMP-3 in 100 µl incubation buffer B1 (50mM Tris-HCl, 125 mM NaCl, 5 mM H_2OCaCl_2, pH 7.5) and incubated 1 h or 5 h at 37°C. In the case of thrombin, 70 µg of total protein of PFC pool were combined with 1 U of enzyme in 50 µl buffer B2 (20 mM Tris-HCl, 0.15 M NaCl, 2.5 mM H_2OCaCl_2, pH 8.4) and incubated 15 h at 37°C. 400 ng and 20 ng of human recombinant hevin (R&D Systems, 2728-SL) were used as positive controls for ADAMTS4/MMP-3 and thrombin digestions, respectively. For negative controls, samples were treated in the same way but without the enzyme. In all cases, the reaction was stopped by addition of PMSF 2 mM, DTT 100 mM, Laemmli buffer (2% SDS, 8% glycerol, 0.01% bromophenol blue) and heated 10 min at 75°C, before being analyzed by western blot.

Data analysis

Results are shown in box-and-whiskers plots with the “box” depicting the median and the 25th and 75th quartiles and the “whisker” showing the 5th and 95th percentile. All statistical calculations were performed using GraphPad Prism 7®. Prior to analysis, all data sets were tested for two criteria: (i) normal distribution and (ii) equality of variances. The normal distribution was tested by applying a D’Agostino & Pearson normality test. The equality of variances was tested with an F-test. In the case of normal distribution and of equal variances, statistical comparisons were made with Student’s unpaired t test. Otherwise, non-parametric tests were used as detailed below. All used statistical models were fixed-effect models. Results were considered statistically significant when p value < 0.05. Significance levels are symbolized with asterisks if $p < 0.05$ (*), $p < 0.01$ (**) or $p < 0.001$ (***).

Subcellular and regional expression pattern for both full-length forms of hevin at ~130 and ~100 kDa. Comparison of hevin levels in total homogenates, cytosolic and membrane-enriched (P2) fraction, and in prefrontal cortex, hippocampus, caudate nucleus and cerebellum were performed from brain samples of 6 individuals (n = 6). Because these data displayed a non-parametric distribution, they were analyzed with a Kruskal-Wallis test followed by a Dunn’s multiple comparisons test.

Sex differences on the expression of hevin bands. The data set composed of 29 PFC samples from 11 females and 18 males passed the normality test, and had equal variance. Student’s unpaired t test was used and showed no significant differences.

Correlation with Age, PMD, storage time and hevin isoform levels. A simple linear regression analysis was performed to determine the correlation between hevin isoform levels and age, PMD, storage time and in between isoforms. No significant correlation was observed except between hevin isoform ($r = 0.8313$, $p \leq 0.0001$).

Astrocytoma and meningioma. Full-length forms of hevin at ~130 and ~100 kDa in astrocytoma (n = 3), meningioma (n = 3) and prefrontal cortex (n = 6) did not passed normality test. These data were analyzed with Mann-Whitney tests.

RESULTS

Specificity of hevin immunoreactivity

Three antibodies against hevin were tested for specificity by western blotting on human PFC total homogenate pool. Anti-human hevin antibody (R&D systems, AF2728) showed two marked bands at the expected molecular weight (Fig. 1A, left), while neither anti-mouse hevin (R&D Systems, AF2836) nor anti-human hevin (Santa Cruz, sc-514275) antibodies showed specific immunoreactivity at the expected size (Fig. 1B, C). Hevin immunoreactive upper band migrated at 130 kDa and the lower band at around 100 kDa, similar to what has been described by other authors (Brekken et al., 2004; Johnston et al., 1990; Kucukdereli et al., 2011; Lively & Brown, 2008a; Lively & Brown, 2008b; Mendis, 1996b; Weaver et al., 2010; Weaver et al., 2011). Intensity of the immunoblot signal increased in a dose-dependent manner (Fig. 1A, right), suggesting specificity. These two bands also appeared when the recombinant hevin protein was loaded (Fig. 1D) and their immunoreactivity was blocked by preincubating the antibody with the blocking peptide (recombinant human hevin, R&D systems, Fig. 1D), supporting the specificity of both bands corresponding to hevin. In addition, we performed western blot experiments on cell extracts and its extracellular medium of BON cells transfected with mouse hevin. Hevin immunoreactivity was detected in hevin-transfected cells and its extracellular medium, but not in mock-transfected cells (Fig. 1E). To further assess the specificity of the selected antibody (R&D AF2728), immunoprecipitation of hevin from PFC total homogenate samples revealed the same bands (~130 and ~100 kDa), which were absent with control IgGs (Fig. 1F). To further assess the specificity of the selected antibody (R&D AF2728), immunoprecipitation of hevin from PFC total homogenate samples revealed the same bands (~130 and ~100 kDa), which were absent with control IgGs (Fig. 1F). Importantly, protein bands at these molecular weights were removed and analyzed by LC-MS/MS, which unambiguously identified hevin protein (UniProtKB Q14515) in both ~130 and ~100 kDa bands (sequence coverage 36 and 18% respectively). Although more unique peptides were found in ~130 kDa band (19 vs 8, probably due to a higher amount of the ~130 kDa isoform), all but one peptide found in the 100 kDa isoforms are common to the ~130 kDa and encompassed almost the entire protein sequence from amino acids A47 to R629 (Supplementary Figure). This proteomic analysis suggests that the 30 kDa difference observed between the two bands are not splicing variants but the result of differential post-translational modifications. Finally, in total homogenates of mouse brain samples, we observed hevin immunoreactivity at ~120 kDa with both anti-mouse hevin (R&D Systems, AF2836) and anti-human hevin (R&D Systems, AF2728) antibodies (Fig. 1G), which was absent in hevin knockout mice. Altogether, these results demonstrate the specificity of the R&D anti-human hevin antibody. We selected this antibody to further characterize hevin protein in human brain tissue.

Deglycosylation, endogenous proteolysis and proteases digestion assays

We determined to study the glycosylation pattern of hevin, its endogenous proteolytic degradation, and its proteolysis by matrix metalloproteases. Firstly, several deglycosylation assays were carried out in order to gain more insight into the structure of the carbohydrate moieties of each of the hevin bands observed in human brain. Human PFC total homogenate pool and human recombinant hevin (R&D Systems, AF2728) were incubated in the presence of PNGase F, EndoF3 or EndoH deglycosylases, enzymes that

remove different types of N-glycosylations. PNGase F (almost all N-glycan, asparagine-linked chains hydrolyzing enzyme (Maley et al., 1989): high mannose, hybrid, bi-, tri- and tetra-antennary) produced a marked shift in both hevin bands of PFC and recombinant protein, leading to lower molecular weight bands of ~125 and ~90 kDa (Fig. 2A-B). These results indicate that both hevin bands are glycosylated proteins. EndoF3 (asparagine-linked fucosylated-bi-antennary and tri-antennary complex oligosaccharides cleaving enzyme) (Maley et al., 1989) seemed to produce a slight shift of both bands in PFC and recombinant protein to lower molecular weight bands, although not as pronounced as PNGaseF. And finally, in the presence of EndoH enzyme (high mannose cleaving enzyme (Maley et al., 1989), only a fraction of the ~130 kDa band suffered a migration shift in both PFC and recombinant protein, which might suggest that this apparent unique band corresponds to a mix of slightly different isoforms or is even a doublet (Fig. 2A-B). Altogether these results confirm that both hevin bands in human brain are glycosylated but in different manner, as in rodent brain (Johnston et al., 1990).

Second, we wanted to determine if the ~100 kDa band derived from the ~130 kDa band via proteolytic degradation. We incubated PFC total homogenate samples at 37°C in the absence of protease inhibitors for a range of times, then denatured the samples at 95°C for 5 min and immediately processed them by western blot. Immunoreactive intensity of the bands was remained unchanged throughout the entire 3 h experiment (Fig. 3A), suggesting the absence of endogenous proteolysis. We next tested the effect of increasing temperatures on hevin proteolysis. PFC total homogenate samples were incubated for 15 min in temperature ranging from 4 to 95°C, then immediately processed for western blot. Temperature-dependent proteolysis did not alter the intensity of the two bands (Fig. 3B). These results suggest that the lower ~100 kDa band is not a degradation product of the ~130 kDa band.

The matrix metalloproteases ADAMTS4, MMP-3 and thrombin have been described to cleave hevin in rodent brains resulting in a C-terminal SPARC-like fragment (SLF), which shares a high homology with SPARC, a close homologue of hevin, and which antagonizes hevin´s synaptogenic function (Weaver et al., 2010; Weaver et al., 2011). To confirm the sensitivity of human hevin towards ADAMTS4, MMP-3 and thrombin, we preformed proteolysis assays incubating PFC pool preparations and human recombinant hevin with the three proteases. As expected, incubation with ADAMTS4 or MMP-3 enzymes in human PFC led to a marked decreased in the intensity of the ~130 kDa and ~100 kDa bands with a concomitant appearance of an intense ~40 kDa double band (Fig. 4A, arrow), that seems to correspond to the SLF fragment (Weaver et al., 2010; Weaver et al., 2011). Likewise, proteolysis of human recombinant hevin decreased the intensity of full-length hevin protein bands. Surprisingly, the band corresponding to the hypothesized SLF had slightly greater molecular weight (Fig. 4A, filled arrowhead). In contrast, hevin proteolytic cleavage by thrombin in both PFC and recombinant proteins, which decreased levels of the ~130 kDa and ~100 kDa bands, produced many fragments higher than 50 kDa (Fig. 4B). In both ADAMTS4 (Fig. 5) and MMP-3 (Fig. 6) dependent-proteolysis assays, pronounced effects were observed when increasing the incubation time (1 h or 5 h of incubation). Importantly, the SLF fragment was identified in non-digested PFC samples, although it showed lower intensity level compared to the ~130 kDa and ~100 kDa bands (Fig. 4A, open arrowhead).

Subcellular and regional distribution of hevin in the human brain

We studied the subcellular distribution of both full-length forms of hevin at ~130 and ~100 kDa in human brain by western blot using cellular fractionation of brain samples into both a cytosolic and a membrane-enriched (P2) fraction. The expression of stathmin and IKβα (NFKB inhibitor alpha) in the cytosolic fraction, together with the enrichment of syntaxin1A, VGLUT1 (Vesicular glutamate transporter 1), NR2A (N-methyl D-aspartate receptor subtype 2A) and PSD95 (postsynaptic density protein 95) and in P2

neuronal membranes confirmed the correct fractionation of brain preparations (Fig. 7). Both hevin ~130 and ~100 kDa bands were strongly enhanced in the membrane-enriched P2 fraction compared to the cytosolic fraction. This subcellular expression pattern was observed in all brain areas (Fig. 8A-D).

For each subcellular fraction (total homogenate, cytosols and P2), similar regional distribution was observed for the ~130 and ~100 kDa hevin forms, i.e. PFC showed the highest expression of hevin bands in all cases (Fig. 9A-C). In addition, greater levels were detected in ~130 kDa and ~100 kDa bands of total homogenate and ~100 kDa band of cytosol fractions in CAU compared to CB ($p<0.05$, $p<0.01$ and $p<0.01$, respectively); and in ~100 kDa band of cytosol in HIP compared to CB ($p<0.05$).

Effect of sex, age, PMD and storage time on hevin immunoreactivity.

To test for sex and age differences on the expression of hevin bands, a larger control cohort of 29 PFC samples, composed of 11 females and 18 males ranging from 18 to 71 years old, was analyzed. Neither sex (11 females vs 18 males), nor age (18–71 years) showed significant differences or correlation with the immunoreactivity of any of the two detected bands (sex ~130 kDa band $p= 0.3544$; ~100 kDa band $p= 0.9787$; age ~130 kDa $p= 0.9248$ and ~100 kDa $p= 0.0514$; Fig. 10A-D). Importantly, no correlation was observed between hevin expression levels and *postmortem* delay (3-39 h) and storage time (18-244 months; PMD ~130 kDa $p= 0.5809$ and ~100 kDa $p= 0.3022$; storage time ~130 kDa $p= 0.5252$ and ~100 kDa $p= 0.9477$; Fig. 10E-H). Interestingly, analyzing this larger control cohort there was found to be a positive correlation between the ~130 kDa and ~100 kDa bands in human PFC ($p< 0.0001$), indicating that subjects that showed high levels for one form also showed high levels for the other and conversely (Fig. 10I).

Hevin expression in astrocytomas, meningiomas, CSF and blood.

Next the relative contribution of the two forms of hevin in astrocytoma tumors (n=3) in comparison with meningioma brain tumors (n=3) were evaluated. Hevin protein expression, clearly detectable in both tumors, was significantly increased in astrocytoma tumors compared with meningioma tumors (~130 kDa band: astrocytoma 200% ± 37 and meningioma 15% ± 7; ~100 kDa band: astrocytoma 121% ± 44 and meningioma 4% ± 1; Fig. 11A). However, the relative expression of the ~130 kDa and ~100 kDa bands (calculated as the 130/100 ratio) was similar in both brain tumors (astrocytoma 34 ± 9 and meningioma 47 ± 13). In contrast, the relative 130/100 hevin bands ratio seems to be increased in both tumor types compared to control PFC brain regions (ratio of 6 ± 1, and $p= 0.002$ in both cases).

Hevin protein expression was also detected in CSF (n=4) and serum (n=4), with apparent higher levels in the CSF (Fig. 11B). Significantly, a new pattern of hevin immunoreactivity was observed in both fluids. A shorter novel band of ~90 kDa band and the ~130 kDa band were detected, without the ~100 kDa band (Fig. 11B).

The presence of hevin in the serum raises the question of its source of expression. We tested the expression of hevin in different blood fractions (serum, platelets, erythrocytes and leucocytes) in order to assess if hevin is produced by blood cells or derives from other organs that would secrete it. Western blot analysis revealed that hevin, which was highly expressed in serum, was absent in any blood cell fraction (~130 kDa and ~90 kDa bands; Fig. 11C), suggesting that hevin is transported into the bloodstream and not synthesized by any blood cell type.

DISCUSSION

In recent years, a number of glycoproteins that constitute the extracellular matrix have been shown to participate in synaptic function (Trinidad et al., 2012). These matricellular proteins are often secreted by

astrocytes and play essential roles during development in synapse formation and plasticity. Among these matricellular proteins, hevin function has been well characterized during development (Eroglu, 2009; Kucukdereli et al., 2011; Lively & Brown, 2008b; Lloyd-Burton & Roskams, 2012; Mendis, 1996a; Mendis et al., 1996b; Mendis et al., 2000; Risher et al., 2014), but its level remains high during adulthood, suggesting a physiological role in adult synaptic plasticity (Johnston et al., 1990; Lively et al., 2007; Lively & Brown, 2008b; Lively & Brown, 2010; Mendis et al., 1996a; Mongrédien et al., 2019). In rodents, astrocytic secretion of hevin is increased after brain injury (Lively et al., 2011; McKinnon & Margolskee, 1996; Mendis et al., 2000) and hevin expression is altered in models of neuropsychiatric disorders (Purcell et al., 2001; Yin et al., 2009). In humans, hevin has also been associated with several mental disorders (Yin et al., 2009; Zhurov et al., 2012). In this context, it is crucial to better characterize hevin protein expression in the human brain. Here, we provide a detailed characterization of hevin protein expression by western blot in *postmortem* adult human brain.

The reliability of our western blot results rests on a thorough validation of the specificity of the selected antibody. Immunodetection of hevin in *postmortem* human brain disappeared when the antibody was previously incubated with the blocking peptide, and was absent in mock-transfected cells and hevin knockout mouse brain lysate. Conversely, hevin signal increased in a protein-dependent manner and after antibody immunoprecipitation. In our study, two main hevin immunoreactive bands were detected in human brain, an intense band of ~130 kDa and a lower molecular weight band of ~100 kDa, which agrees to a great extent with previous results in the literature. Hevin immunoreactivity has mostly been described as a 116/120 kDa doublet in rat brain (Johnston et al., 1990; Lively & Brown, 2008a; Lively & Brown, 2008b; Mendis et al., 1996a), but ~130 kDa and 105 kDa hevin bands have also been described in human and mouse brain lysates (Brekken et al., 2004; Kucukdereli et al., 2011; Weaver et al., 2010).

In order to further investigate the nature of the main hevin bands, we performed several biochemical assays. Time- and temperature- dependent proteolysis assays discharged ~100 kDa hevin form as the degradation product of the ~130 kDa form. Hevin is a 664 amino-acids glycoprotein composed of a signal peptide, an acidic N-terminal domain, followed by a follistatin-like domain and an extracellular Ca^{2+} binding-domain at the C-terminus. Several potential N-glycosylation sites have been proposed along hevin's protein sequence, mainly in the acidic N-terminal and in the follistatin-like domain (Asn-444) (Bendik et al., 1998; Girard & Springer, 1995; Hambrock et al., 2003). Additionally, several O-glycosylation sites have also been experimentally observed in human CSF (Halim et al., 2013). Our deglycosylation assays demonstrated that both hevin forms in human brain are N-glycosylated (PNGaseF cleavage). In both bands, some glycosylations corresponded to bi-antennary or tri-antennary fucosylation (EnfoF3 cleavage, but less migration shift than PNGaseF), while some N-glycosylation were due to N-linked high-mannose hybrid glycosylation (EndoH cleavage) only in the ~130 kDa form (Freeze & Kranz, 2010). PNGaseF deglycosylation leads to a ~90 kDa band, which may correspond to native hevin -with a calculated theoretical Mw of ~71 kDa (Johnston et al., 1990), or to some form of hevin with other post-translational modifications such as phosphorylation. These results concord with those described in rat brain lysates and mouse recombinant hevin (Hambrock et al., 2003; Johnston et al., 1990). The expression of two post-translationally distinct forms of hevin in different species suggests a conserved role in adult physiological brain function.

Proteolysis of hevin by ADAMTS4, MMP-3 and thrombin liberates the C terminus portion of mouse and recombinant hevin (amino-acids 350-650), which possess 60 % of identity to SPARC, and hence was named SPARC-like fragment (SLF) (Kucukdereli et al., 2011; Weaver et al., 2010; Weaver et al., 2011). SLF, like SPARC, antagonizes the synaptogenic activity of hevin (Kucukdereli et al., 2011). Here we

confirmed that human hevin is cleaved by these 3 enzymes. Incubation of human PFC total homogenate samples with ADAMTS4 or MMP-3 produced a double band with similar molecular weight (~40 kDa) to that described in mouse brain (Weaver et al., 2010; Weaver et al., 2011). By contrast, the cleaved product of the recombinant human hevin was larger (~47 kDa). Differences in post-translational modifications in hevin PFC or recombinant protein (in this case produced in a mouse myeloma cell line) could explain the observed molecular weight differences of the cleaved product. Hevin proteolysis by thrombin produced very different molecular weight fragments in both PFC and recombinant proteins, due to thrombin non-specific cleavage sites (Rajalingam et al., 2008). Regardless of the protease identity, *in vivo* digestion of hevin occurs as we could detect the hypothetical SLF fragment in non-digested PFC samples, despite very low levels compared to full-length hevin. Biochemical studies in ADAMTS4-null mice suggest that hevin is endogenously digested primarily by ADAMTS4 at least in the cerebellum (Weaver et al., 2010). Future studies are needed to identify the proteases responsible for the cleavage of hevin in human brain. Based on the antagonistic role of SLF on hevin synaptogenic function, it would be relevant to include the quantification of SLF levels along with hevin in future studies on human neuropsychiatric disorders.

Consistent with the wealth of experimental evidences showing hevin expression in synaptic junctions (Hambrock et al., 2003; Johnston et al., 1990; Singh et al., 2016), we found that the two human hevin forms, ~130 kDa and ~100 kDa, are strongly enriched in membranous fraction compared to cytosolic preparations in all brain region tested. The enrichment in membrane preparation suggests that hevin is trapped in the complex mesh-like matrix of the synapses. However, hevin's presence in the cytosolic (soluble) fraction reflects its soluble nature and also suggests that it can also attach to different targets before being secreted to the ECM (Ge et al., 2020; Hambrock et al., 2003; Sullivan et al., 2006). Additionally, the two human hevin immunoreactive bands were detected in the four brain regions studied with the largest expression detected in the PFC. This data is similar to the regional expression of hevin mRNA shown in mouse brain, with a strong expression in cortical regions (Mongrédien et al., 2019). In addition, we have previously observed in adult human brain, hevin mRNA expression in astrocytes and parvalbumin interneurons in PFC and CAU, and in glutamatergic neurons in PFC (Mongrédien et al., 2019). Our present results confirm that hevin mRNA is translated in adult human brain and add evidence for a region-specific expression of hevin. Hevin strong cortical expression suggests a major role in higher cognitive functions such as decision-making, social and emotional behavior, learning and memory. Thus, future analysis of hevin in several limbic brain regions of patients with psychiatric disorders such as depression, drug addiction and schizophrenia would be particularly relevant. In addition, based on recent evidence showing that post-translational modifications are crucial in synaptic functions (Zhang et al., 2018), analysis of hevin expression levels should differentiate between the two isoforms**.**

Besides being expressed in the non-pathological brain, previous studies have demonstrated that hevin protein expression is induced in reactive astrocytes (Jones & Bouvier, 2014; Lively et al., 2011; McKinnon & Margolskee, 1996; Mendis et al., 2000), and abnormal astrocyte activation has been related with tumor formation, such as astrocytoma (Gronseth et al., 2018; Yang et al., 2013). Upregulated hevin mRNA expression has also been reported in human meningiomas or meningeal tumors (Dalan et al., 2017), which are typically slow-growing tumors of the meninges, where the arachnoid mater cells transform into meningioma cells (Buerki et al., 2018; Fathi & Roelcke, 2013). However, these studies did not distinguish between the different hevin forms. Here we show that astrocytoma samples exhibited greater hevin immunoreactivity than meningioma samples, in both hevin bands. However no significant differences in the relative expression of the ~130 kDa and ~100 kDa bands (ratio) were detected between both types of tumors. These results are consistent with the well-known role of hevin and other ECM molecules in tumor invasion, and the proposal of hevin as a marker of glioblastoma and astrocytoma

progression (He et al., 2016; Turtoi et al., 2012; Virga et al., 2018). Nevertheless, the fact that hevin expression is downregulated in other types of human cancers, has suggested it may play different roles in tumor biology, as both oncogene and tumor suppressor, based on tumor type (Gagliardi et al., 2017). Hevin's implication in cell adhesion, migration and proliferation highlight its role as a key protein in the regulation of tumor biology (Claeskens et al., 2000; Gagliardi et al., 2017).

Finally, we evaluated hevin expression pattern in CSF and blood samples. It has been shown that hevin protein is upregulated in the CSF of multiple sclerosis patients, while it is absent in normal CSF in the same study (Hammack et al., 2004). In contrast to that study, herein we demonstrate that two hevin forms are secreted into the CSF in subjects without psychiatric or neurological disorders. However, the origin of CSF hevin remains unknown; it may originate from brain's astrocytes and/or neurons, meninges or anywhere in the periphery and arrive by bloodstream. In addition, although we clearly detected hevin in blood plasma, none of the blood cell expressed it (platelets, erythrocytes and leucocytes), suggesting that hevin present in blood derives from other organs where hevin is expressed such as brain, endothelial cells of high endothelial venules (Girard & Springer, 1995, 1996), liver (Klingler et al., 2020), stomach (Klingler et al., 2020), small intestine (Klingler et al., 2020), oesophagus (Klingler et al., 2020), lung (Bendik et al., 1998; Klingler et al., 2020; Weaver et al., 2010), pancreas (Bendik et al., 1998; Weaver et al., 2010), heart (Bendik et al., 1998; Johnston et al., 1990; Weaver et al., 2011), spleen or kidney (Bendik et al., 1998; Soderling et al., 1997). Interestingly, it was noted that, while ~130 kDa band was present in both CSF and serum, the ~100 kDa band was absent and a ~90 kDa band was detected. This band may correspond to non-glycosylated form, as shown in deglycosylation assays. The different proportion of the two detected hevin forms in CSF and in blood suggests a different glycosylation/deglycosylation pattern and/or a different source of origin for hevin in each fluid (Barone et al., 2012; Karlsson et al., 2017).

The present study provides a thorough characterization of hevin protein expression by western blot in *postmortem* human brain. The data herein presented reveal that there are two forms of hevin, both glycosylated, whose expression is higher in the membrane-enriched fraction compared to the cytosolic/soluble fraction. Furthermore, hevin expression is higher in the PFC in comparison to other brain regions. Hevin protein in PFC did not vary with age, nor sex. It is also shown that hevin is expressed in human CSF and blood plasma, but not in blood cells. Taken together, these results constitute an essential resource for future studies of hevin in brain tissue under pathological and non-pathological conditions.

REFERENCES

Barone, R., Sturiale, L., Palmigiano, A., Zappia, M., & Garozzo, D. (2012). Glycomics of pediatric and adulthood diseases of the central nervous system. *Journal of Proteomics*, *75*(17), 5123–5139. https://doi.org/10.1016/j.jprot.2012.07.007

Bendik, I., Schraml, P., & Ludwig, C. U. (1998). Characterization of MAST9/Hevin, a SPARC-like Protein, That is Down-Regulated in Non-Small Cell Lung Cancer. *Cancer Research*, *58*(4), 626–629.

Bornstein P. Diversity of function is inherent in matricellular proteins: An appraisal of thrombospondin 1. (1995). *The Journal of Cell Biology*, *130*(3), 503–506.

Bornstein, P. (2009). Matricellular proteins: An overview. *Journal of Cell Communication and Signaling*, *3*(3–4), 163–165. https://doi.org/10.1007/s12079-009-0069-z

Bornstein, P., & Sage, E. H. (2002). Matricellular proteins: Extracellular modulators of cell function. *Current Opinion in Cell Biology*, *14*(5), 608–616. https://doi.org/10.1016/S0955-0674(02)00361-7

Bradford, M. M. (1976). A rapid and sensitive method for the quantitation of microgram quantities of protein utilizing the principle of protein-dye binding. *Analytical Biochemistry*, *72*(1), 248–254. https://doi.org/10.1016/0003-2697(76)90527-3

Brekken, R. A., Sullivan, M. M., Workman, G., Bradshaw, A. D., Carbon, J., Siadak, A., Murri, C., Framson, P. E., & Sage, E. H. (2004). Expression and Characterization of Murine Hevin (SC1), a Member of the SPARC Family of Matricellular Proteins. *Journal of Histochemistry & Cytochemistry*, *52*(6), 735–748. https://doi.org/10.1369/jhc.3A6245.2004

Brocos-Mosquera, I., Nuñez Del Moral, A., Morentin, B., Meana, J. J., Callado, L. F., & Erdozain, A. M. (2018). Characterisation of spinophilin immunoreactivity in postmortem human brain homogenates. *Progress in Neuro-Psychopharmacology & Biological Psychiatry*, *81*, 236–242. https://doi.org/10.1016/j.pnpbp.2017.09.019

Buerki, R. A., Horbinski, C. M., Kruser, T., Horowitz, P. M., James, C. D., & Lukas, R. V. (2018). An overview of meningiomas. *Future Oncology*, *14*(21), 2161–2177. https://doi.org/10.2217/fon-2018-0006

Claeskens, A., Ongenae, N., Neefs, J. M., Cheyns, P., Kaijen, P., Cools, M., & Kutoh, E. (2000). Hevin is down-regulated in many cancers and is a negative regulator of cell growth and proliferation. *British Journal of Cancer*, *82*(6), 1123–1130. https://doi.org/10.1054/bjoc.1999.1051

Collins, M. A., An, J., Peller, D., & Bowser, R. (2015). Total protein is an effective loading control for cerebrospinal fluid western blots. *Journal of Neuroscience Methods*, *251*, 72–82. https://doi.org/10.1016/j.jneumeth.2015.05.011

Correia, S. C., Carvalho, C., Cardoso, S., & Moreira, P. I. (2019). Post-translational modifications in brain health and disease. *Biochimica et Biophysica Acta (BBA) - Molecular Basis of Disease*, *1865*(8), 1947–1948. https://doi.org/10.1016/j.bbadis.2019.05.006

Dalan, A. B., Gulluoglu, S., Tuysuz, E. C., Kuskucu, A., Yaltirik, C. K., Ozturk, O., Ture, U., & Bayrak, O. F. (2017). Simultaneous analysis of miRNA-mRNA in human meningiomas by integrating transcriptome: A relationship between PTX3 and miR-29c. *BMC Cancer*, *17*(1), 207. https://doi.org/10.1186/s12885-017-3198-4

Elu, N., Osinalde, N., Beaskoetxea, J., Ramirez, J., Lectez, B., Aloria, K., Rodriguez, J. A., Arizmendi, J. M., & Mayor, U. (2019). Detailed Dissection of UBE3A-Mediated DDI1 Ubiquitination. *Frontiers in Physiology*, *10*, 534. https://doi.org/10.3389/fphys.2019.00534

Eroglu, C. (2009). The role of astrocyte-secreted matricellular proteins in central nervous system development and function. *Journal of Cell Communication and Signaling*, *3*(3–4), 167–176. https://doi.org/10.1007/s12079-009-0078-y

Fathi, A.-R., & Roelcke, U. (2013). Meningioma. *Current Neurology and Neuroscience Reports*, *13*(4). https://doi.org/10.1007/s11910-013-0337-4

Freeze, H. H., & Kranz, C. (2010). Endoglycosidase and Glycoamidase Release of N-Linked Glycans. *Current Protocols in Molecular Biology*, *89*(1), 17. https://doi.org/10.1002/0471142727.mb1713as89

Gagliardi, F., Narayanan, A., & Mortini, P. (2017). SPARCL1 a novel player in cancer biology. *Critical Reviews in Oncology/Hematology*, *109*, 63–68. https://doi.org/10.1016/j.critrevonc.2016.11.013

Ge, L., Zhuo, Y., Wu, P., Liu, Y., Qi, L., Teng, X., Duan, D., Chen, P., & Lu, M. (2020). Olfactory ensheathing cells facilitate neurite sprouting and outgrowth by secreting high levels of hevin. *Journal of Chemical Neuroanatomy*, *104*, 101728. https://doi.org/10.1016/j.jchemneu.2019.101728

Girard, J.-P., & Springer, T. A. (1995). Cloning from purified high endothelial venule cells of hevin, a close relative of the antiadhesive extracellular matrix protein SPARC. *Immunity*, *2*(1), 113–123. https://doi.org/10.1016/1074-7613(95)90083-7

Girard, J.-P., & Springer, T. A. (1996). Modulation of Endothelial Cell Adhesion by Hevin, an Acidic Protein Associated with High Endothelial Venules. *Journal of Biological Chemistry*, *271*(8), 4511–4517. https://doi.org/10.1074/jbc.271.8.4511

Gongidi, V., Ring, C., Moody, M., Brekken, R., Sage, E. H., Rakic, P., & Anton, E. S. (2004). SPARC-like 1 regulates the terminal phase of radial glia-guided migration in the cerebral cortex. *Neuron*, *41*(1), 57–69.

Gronseth, E., Wang, L., Harder, D. R., & Ramchandran, R. (2018). The Role of Astrocytes in Tumor Growth and Progression. *Astrocyte - Physiology and Pathology*. https://doi.org/10.5772/intechopen.72720

Halim, A., Rüetschi, U., Larson, G., & Nilsson, J. (2013). LC–MS/MS Characterization of O-Glycosylation Sites and Glycan Structures of Human Cerebrospinal Fluid Glycoproteins. *Journal of Proteome Research*, *12*(2), 573–584. https://doi.org/10.1021/pr300963h

Hambrock, H. O., Nitsche, D. P., Hansen, U., Bruckner, P., Paulsson, M., Maurer, P., & Hartmann, U. (2003). SC1/Hevin: An Extracellular Calcium-Modulated Protein That Binds Collagen I. *Journal of Biological Chemistry*, *278*(13), 11351–11358. https://doi.org/10.1074/jbc.M212291200

Hammack, B. N., Fung, K. Y. C., Hunsucker, S. W., Duncan, M. W., Burgoon, M. P., Owens, G. P., & Gilden, D. H. (2004). Proteomic analysis of multiple sclerosis cerebrospinal fluid. *Multiple Sclerosis (Houndmills, Basingstoke, England)*, *10*(3), 245–260. https://doi.org/10.1191/1352458504ms1023oa

Hashimoto, N., Sato, T., Yajima, T., Fujita, M., Sato, A., Shimizu, Y., Shimada, Y., Shoji, N., Sasano, T., & Ichikawa, H. (2016). SPARCL1-containing neurons in the human brainstem and sensory ganglion. *Somatosensory & Motor Research*, *33*(2), 112–117. https://doi.org/10.1080/08990220.2016.1197115

He, X., Lee, B., & Jiang, Y. (2016). Cell-ECM Interactions in Tumor Invasion. In K. A. Rejniak (Ed.), *Systems Biology of Tumor Microenvironment* (Vol. 936, pp. 73–91). Springer International Publishing. https://doi.org/10.1007/978-3-319-42023-3_4

Jones, E. V., & Bouvier, D. S. (2014). *Astrocyte-Secreted Matricellular Proteins in CNS Remodelling during Development and Disease.*. Neural Plasticity. 321209. https://doi.org/10.1155/2014/321209

Johnston, I. G., Paladino, T., Gurd, J. W., & Brown, I. R. (1990). Molecular cloning of SC1: A putative brain extracellular matrix glycoprotein showing partial similarity to osteonectin/BM40/SPARC. *Neuron*, *4*(1), 165–176. https://doi.org/10.1016/0896-6273(90)90452-L

Karlsson, I., Ndreu, L., Quaranta, A., & Thorsén, G. (2017). Glycosylation patterns of selected proteins in individual serum and cerebrospinal fluid samples. *Journal of Pharmaceutical and Biomedical Analysis*, *145*, 431–439. https://doi.org/10.1016/j.jpba.2017.04.040

Klingler, A., Regensburger, D., Tenkerian, C., Britzen-Laurent, N., Hartmann, A., Stürzl, M., & Naschberger, E. (2020). Species-, organ- and cell-type-dependent expression of SPARCL1 in human and mouse tissues. *PLOS ONE*, *15*(5), e0233422. https://doi.org/10.1371/journal.pone.0233422

Kucukdereli, H., Allen, N. J., Lee, A. T., Feng, A., Ozlu, M. I., Conatser, L. M., Chakraborty, C., Workman, G., Weaver, M., Sage, E. H., Barres, B. A., & Eroglu, C. (2011). Control of excitatory CNS synaptogenesis by astrocyte-secreted proteins Hevin and SPARC. *Proceedings of the National Academy of Sciences of the United States of America*, *108*(32), E440-449. https://doi.org/10.1073/pnas.1104977108

Lively, S., & Brown, I. R. (2008a). Extracellular matrix protein SC1/hevin in the hippocampus following pilocarpine-induced status epilepticus. *Journal of Neurochemistry*, *107*(5), 1335–1346. https://doi.org/10.1111/j.1471-4159.2008.05696.x

Lively, S., & Brown, I. R. (2008b). Localization of the Extracellular Matrix Protein SC1 Coincides with Synaptogenesis During Rat Postnatal Development. *Neurochemical Research*, *33*(9), 1692–1700. https://doi.org/10.1007/s11064-008-9606-z

Lively, S., & Brown, I. R. (2010). The Extracellular Matrix Protein SC1/Hevin Localizes to Multivesicular Bodies in Bergmann Glial Fibers in the Adult Rat Cerebellum. *Neurochemical Research*, *35*(2), 315–322. https://doi.org/10.1007/s11064-009-0057-y

Lively, S., Moxon-Emre, I., & Schlichter, L. C. (2011). SC1/hevin and reactive gliosis after transient ischemic stroke in young and aged rats. *Journal of Neuropathology and Experimental Neurology*, *70*(10), 913–929. https://doi.org/10.1097/NEN.0b013e318231151e

Lively, S., Ringuette, M. J., & Brown, I. R. (2007). Localization of the Extracellular Matrix Protein SC1 to Synapses in the Adult Rat Brain. *Neurochemical Research*, *32*(1), 65–71. https://doi.org/10.1007/s11064-006-9226-4

Lloyd-Burton, S., & Roskams, A. J. (2012). SPARC-like 1 (SC1) is a diversely expressed and developmentally regulated matricellular protein that does not compensate for the absence of SPARC in the CNS. *The Journal of Comparative Neurology*, *520*(12), 2575–2590. https://doi.org/10.1002/cne.23029

Maley, F., Trimble, R. B., Tarentino, A. L., & Plummer, T. H. (1989). Characterization of glycoproteins and their associated oligosaccharides through the use of endoglycosidases. *Analytical Biochemistry*, *180*(2), 195–204. https://doi.org/10.1016/0003-2697(89)90115-2

McKinnon, P. J., & Margolskee, R. F. (1996). SC1: A marker for astrocytes in the adult rodent brain is upregulated during reactive astrocytosis. *Brain Research*, *709*(1), 27–36. https://doi.org/10.1016/0006-8993(95)01224-9

McKinnon, P. J., McLaughlin, S. K., Kapsetaki, M., & Margolskee, R. F. (2000). Extracellular Matrix-Associated Protein Sc1 Is Not Essential for Mouse Development. *Molecular and Cellular Biology*, *20*(2), 656–660. https://doi.org/10.1128/MCB.20.2.656-660.2000

Mendis, D. B., Shahin, S., Gurd, J. W., & Brown, I. R. (1996a). SC1, A SPARC-related glycoprotein, exhibits features of an ECM component in the developing and adult brain. *Brain Research*, *713*(1–2), 53–63. https://doi.org/10.1016/0006-8993(95)01472-1

Mendis, D. B., Ivy, G. O., & Brown, I. R. (1996b). SC1, a brain extracellular matrix glycoprotein related to SPARC and follistatin, is expressed by rat cerebellar astrocytes following injury and during development. *Brain Research*, *730*(1–2), 95–106. https://doi.org/10.1016/S0006-8993(96)00440-4

Mendis, D. B., Ivy, G. O., & Brown, I. R. (2000). Induction of SC1 mRNA encoding a brain extracellular matrix glycoprotein related to SPARC following lesioning of the adult rat forebrain. *Neurochemical Research*, *25*(12), 1637–1644. PubMed. https://doi.org/10.1023/a:1026626805612

Mongrédien, R., Erdozain, A. M., Dumas, S., Cutando, L., del Moral, A. N., Puighermanal, E., Rezai Amin, S., Giros, B., Valjent, E., Meana, J. J., Gautron, S., Callado, L. F., Fabre, V., & Vialou, V. (2019). Cartography of hevin-expressing cells in the adult brain reveals prominent expression in astrocytes and parvalbumin neurons. *Brain Structure and Function,* 224(3),1219-1244. https://doi.org/10.1007/s00429-019-01831-x

Murphy-Ullrich, J. E., & Sage, E. H. (2014). Revisiting the matricellular concept. *Matrix Biology : Journal of the International Society for Matrix Biology*, *37*, 1–14. https://doi.org/10.1016/j.matbio.2014.07.005

Nilsson, J., Rüetschi, U., Halim, A., Hesse, C., Carlsohn, E., Brinkmalm, G., & Larson, G. (2009). Enrichment of glycopeptides for glycan structure and attachment site identification. *Nature Methods*, *6*(11), 809–811. https://doi.org/10.1038/nmeth.1392

Purcell, A. E., Jeon, O. H., Zimmerman, A. W., Blue, M. E., & Pevsner, J. (2001). Postmortem brain abnormalities of the glutamate neurotransmitter system in autism. *Neurology*, *57*(9), 1618-1628. https://doi.org/10.1212/WNL.57.9.1618

Rajalingam, D., Kathir, K. M., Ananthamurthy, K., Adams, P. D., & Kumar, T. K. S. (2008). A method for the prevention of thrombin-induced degradation of recombinant proteins. *Analytical Biochemistry*, *375*(2), 361–363. https://doi.org/10.1016/j.ab.2008.01.014

Risher, W. C., Patel, S., Kim, I. H., Uezu, A., Bhagat, S., Wilton, D. K., Pilaz, L.-J., Singh Alvarado, J., Calhan, O. Y., Silver, D. L., Stevens, B., Calakos, N., Soderling, S. H., & Eroglu, C. (2014). Astrocytes refine cortical connectivity at dendritic spines. *ELife*, *3,* e04047. https://doi.org/10.7554/eLife.04047

Shevchenko, A., Wilm, M., Vorm, O., & Mann, M. (1996). Mass Spectrometric Sequencing of Proteins from Silver-Stained Polyacrylamide Gels. *Anal. Chem*., 68(5):850-8. https://doi.org/10.1021/ac950914h

Singh, S. K., Stogsdill, J. A., Pulimood, N. S., Dingsdale, H., Kim, Y. H., Pilaz, L.-J., Kim, I. H., Manhaes, A. C., Rodrigues-Junior, W. S., Pamukcu, A., Enustun, E., Ertuz, Z., Scheiffele, P., Soderling, S., Silver, D. L., Ji, R.-R., Medina, A. E., & Eroglu, C. (2016). Astrocytes Assemble Thalamocortical Synapses by Bridging Nrx1α and NL1 via Hevin. *Cell*, *164*(1-2), 183–196. https://doi.org/10.1016/j.cell.2015.11.034

Soderling, J. A., Reed, M. J., Corsa, A., & Sage, E. H. (1997). Cloning and Expression of Murine SC1, a Gene Product Homologous to SPARC. *Journal of Histochemistry & Cytochemistry*, *45*(6), 823–835. https://doi.org/10.1177/002215549704500607

Sullivan, M. M., Barker, T. H., Funk, S. E., Karchin, A., Seo, N. S., Höök, M., Sanders, J., Starcher, B., Wight, T. N., Puolakkainen, P., & Sage, E. H. (2006). Matricellular Hevin Regulates Decorin Production and Collagen Assembly. *Journal of Biological Chemistry*, *281*(37), 27621–27632. https://doi.org/10.1074/jbc.M510507200

Sullivan, M. M., & Sage, E. H. (2004). Hevin/SC1, a matricellular glycoprotein and potential tumor-suppressor of the SPARC/BM-40/Osteonectin family. *The International Journal of Biochemistry & Cell Biology*, *36*(6), 991–996. https://doi.org/10.1016/j.biocel.2004.01.017

Trinidad, J. C., Barkan, D. T., Gulledge, B. F., Thalhammer, A., Sali, A., Schoepfer, R., & Burlingame, A. L. (2012). Global identification and characterization of both O-GlcNAcylation and phosphorylation at the murine synapse. *Molecular & cellular proteomics : MCP*, *11*(8), 215–229. https://doi.org/10.1074/mcp.O112.018366

Turtoi, A., Musmeci, D., Naccarato, A. G., Scatena, C., Ortenzi, V., Kiss, R., Murtas, D., Patsos, G., Mazzucchelli, G., De Pauw, E., Bevilacqua, G., & Castronovo, V. (2012). Sparc-Like Protein 1 Is a New Marker of Human Glioma Progression. *Journal of Proteome Research*, *11*(10), 5011–5021. https://doi.org/10.1021/pr3005698

Vialou, V., Robison, A. J., Laplant, Q. C., Covington, H. E., 3rd, Dietz, D. M., Ohnishi, Y. N., Mouzon, E., Rush, A. J., Watts, E. L., Wallace, D. L., Iñiguez, S. D., Ohnishi, Y. H., Steiner, M. A., Warren, B. L., Krishnan, V., Bolaños, C. A., Neve, R. L., Ghose, S., Berton, O., Tamminga, C. A.,Nestler, E. J. (2010). DeltaFosB in brain reward circuits mediates resilience to stress and antidepressant responses. *Nature neuroscience*, *13*(6), 745–752. https://doi.org/10.1038/nn.2551

Virga, J., Bognár, L., Hortobágyi, T., Zahuczky, G., Csősz, É., Kalló, G., Tóth, J., Hutóczki, G., Reményi-Puskár, J., Steiner, L., & Klekner, A. (2018). Tumor Grade versus Expression of Invasion-Related Molecules in Astrocytoma. *Pathology & Oncology Research*, *24*(1), 35–43. https://doi.org/10.1007/s12253-017-0194-6

Weaver, M. S., Workman, G., Cardo-Vila, M., Arap, W., Pasqualini, R., & Sage, E. H. (2010). Processing of the Matricellular Protein Hevin in Mouse Brain Is Dependent on ADAMTS4. *Journal of Biological Chemistry*, *285*(8), 5868–5877. https://doi.org/10.1074/jbc.M109.070318

Weaver, M., Workman, G., Schultz, C. R., Lemke, N., Rempel, S. A., & Sage, E. H. (2011). Proteolysis of the matricellular protein hevin by matrix metalloproteinase-3 produces a SPARC-like fragment (SLF) associated with neovasculature in a murine glioma model. *Journal of Cellular Biochemistry*, *112*(11), 3093–3102. https://doi.org/10.1002/jcb.23235

Yang, C., Rahimpour, S., Yu, A. C. H., Lonser, R. R., & Zhuang, Z. (2013). Regulation and dysregulation of astrocyte activation and implications in tumor formation. *Cellular and Molecular Life Sciences: CMLS*, *70*(22), 4201–4211. https://doi.org/10.1007/s00018-013-1274-8

Yin, G. N., Lee, H. W., Cho, J.-Y., & Suk, K. (2009). Neuronal pentraxin receptor in cerebrospinal fluid as a potential biomarker for neurodegenerative diseases. *Brain Research*, *1265*, 158–170. https://doi.org/10.1016/j.brainres.2009.01.058

Zhang, P., Lu, H., Peixoto, R. T., Pines, M. K., Ge, Y., Oku, S., Siddiqui, T. J., Xie, Y., Wu, W., Archer-Hartmann, S., Yoshida, K., Tanaka, K. F., Aricescu, A. R., Azadi, P., Gordon, M. G., Sabatini, B. L., Wong, R. O. L., Craig, A. M. (2018). Heparan Sulfate Organizes Neuronal Synapses through Neurexin Partnerships, *Cell*, 174(6), 1450-1464.e23. https://doi.org/10.1016/j.cell.2018.07.002

Zhurov, V., Stead, J. D. H., Merali, Z., Palkovits, M., Faludi, G., Schild-Poulter, C., Anisman, H., & Poulter, M. O. (2012). Molecular Pathway Reconstruction and Analysis of Disturbed Gene Expression in Depressed Individuals Who Died by Suicide. *PLoS ONE*, *7*(10), e47581. https://doi.org/10.1371/journal.pone.0047581

ACKNOWLEDGEMENTS

Mass spectrometry analysis was performed by Kerman Aloria in the Proteomics Core Facility-SGIKER at the University of the Basque Country (member of ProteoRed-ISCIII).

AUTHOR CONTRIBUTIONS

A.E., L.C. and V.V. conceived the study. L.C. managed and provided the human post-mortem samples. A.N. and I.B. performed brain and blood fractionation. A.N. performed Western blot analysis. V.V. performed mouse brain dissection and mouse Western blot. A.N. and I.B. performed deglycosylation, proteolysis, immunoprecipitation assay. A.N. and A.E. participated in HPLC/MS analysis. L.C. provided key facilities, equipment and advice. A.E. coordinated the study. A.E. and A.N. wrote the manuscript. All authors reviewed and approved the manuscript.

FUNDING SOURCES

This work was supported by The European Fundation for Alcohol Research (ERAB, EA 1819); Basque Government (IT1211-19); Fundación Vital (2018); Brain & Behavior Research Foundation (NARSAD, #17566), FP7 Marie Curie Actions Career Integration Grant (FP7- PEOPLE-2013-CIG #618807), Agence Nationale de la Recherche (ANR JCJC 2015). A. Nuñez-del Moral is recipient of a Predoctoral Fellowship from the Basque Government.

DECLARATIONS OF INTEREST

None.

TABLES

PRIMARY ANTIBODY	TRADING HOUSE	CATALOG NUMBER	ANTIBODY TYPE	IMMUNIZED SPECIE	DILUTION
Anti-human SPARCL1	R&D Systems	AF2728	Polyclonal	Goat	1:3000
Anti-human SPARCL1	Santa Cruz Biotechnology	sc-514275	Monoclonal	Mouse	1:500
Anti-mouse SPARCL1	R&D Systems	AF2836	Polyclonal	Goat	1:2000
Anti-human β-actin	Sigma-aldrich	A1978	Monoclonal	Mouse	1: 100.000
Anti-human Syntaxin1A	Merck Millipore	MAB336	Polyclonal	Mouse	1:2000
Anti-human Vglut1	Donated by S. El Mestikawy	----	Polyclonal	Rabbit	1:1000
Anti-human NR2A	Santa Cruz Biotechnology	sc-1468	Polyclonal	Goat	1:1000
Anti-human PSD95	Merck Millipore	MAB1596	Monoclonal	Mouse	1:1000
Anti-human Stathmin	Cell Signaling Technology	#3352	Polyclonal	Rabbit	1:200
Anti-human Ikb-α	Santa Cruz Biotechnology	Sc-371	Polyclonal	Rabbit	1:500

Table 1. References and dilutions of the primary antibodies used in this study.

TYPE OF ASSAY	SAMPLE NUMBER (N)	AGE (MEAN±SEM)	SEX (FEMALE/MALE)
Antibody specificity, degradation and enzymatic assays	Pool preparation containing samples from 4 different subjects	45±2	4M
Regional and subcellular expression assays	6 PFC 6 HIP 6 CAU 6 CB	44±1	6M
Correlations with different variables	29 PFC	50±2	11F/18M
Astrocytoma	3	49±8	3M
Meningioma	3	61±7	2F/1M
Cerebrospinal fluid	4	65±7	4M
Blood	4	28±3	4F

Table 2. Demographic characteristics and number of the subjects included in each assay of this study.

FIGURES

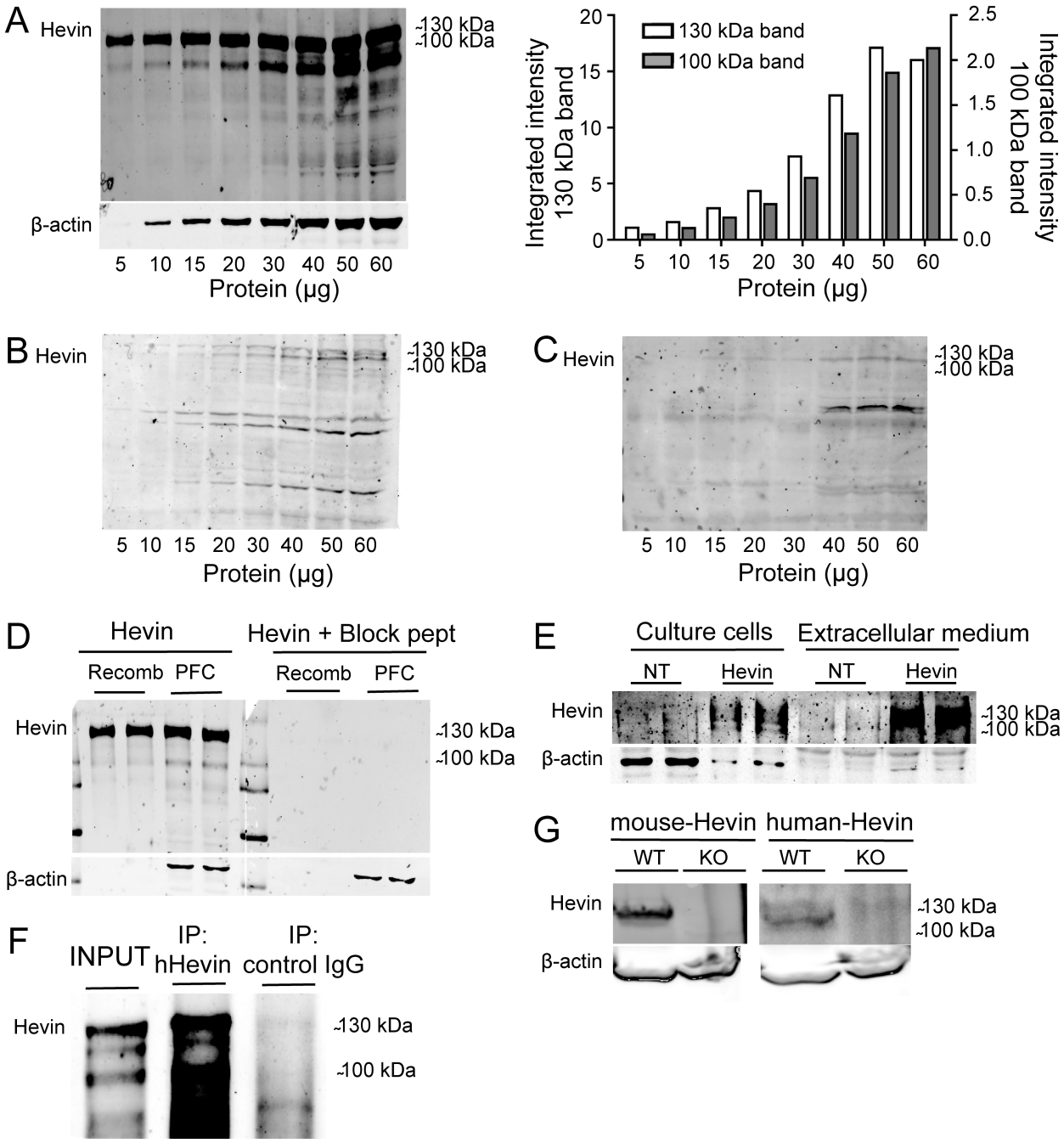

Figure 1. Validation of human hevin antibody specificity. A) Protein dependent-curve of hevin immunoreactivity in PFC total homogenate pool (5-60 µg) with goat anti-human hevin antibody (and the corresponding quantification of ~130 kDa and ~100 kDa hevin bands), B) with goat anti-mouse hevin antibody and C) with mouse anti-human hevin antibody. Blots A, B and C were run in parallel with the same sample and blot A was incubated with ß-actin. D) Hevin immunoreactivity with goat anti-human hevin antibody in PFC total homogenate and in human recombinant hevin (Recomb), in the presence or absence of its blocking peptide. E) Hevin immunoreactivity with goat anti-human hevin antibody in cell culture lysate and in the extracellular medium of mock-transfected (NT) and hevin-tranfected BON cells. F) Immunoblotting with goat anti-human hevin after immunoprecipitating hevin protein with goat anti-human hevin or control IgG in PFC total homogenate. The input loaded in the gel corresponds to 1:20 fraction of the tissue used in the assays. G) Hevin immunoreactivity in wild-type (WT) and hevin knockout (KO) mouse brain homogenates (50 µg), with goat anti-mouse antibody or goat anti-human hevin antibody. Molecular weights are shown on the figure. Samples in panel D and E were run in duplicate.

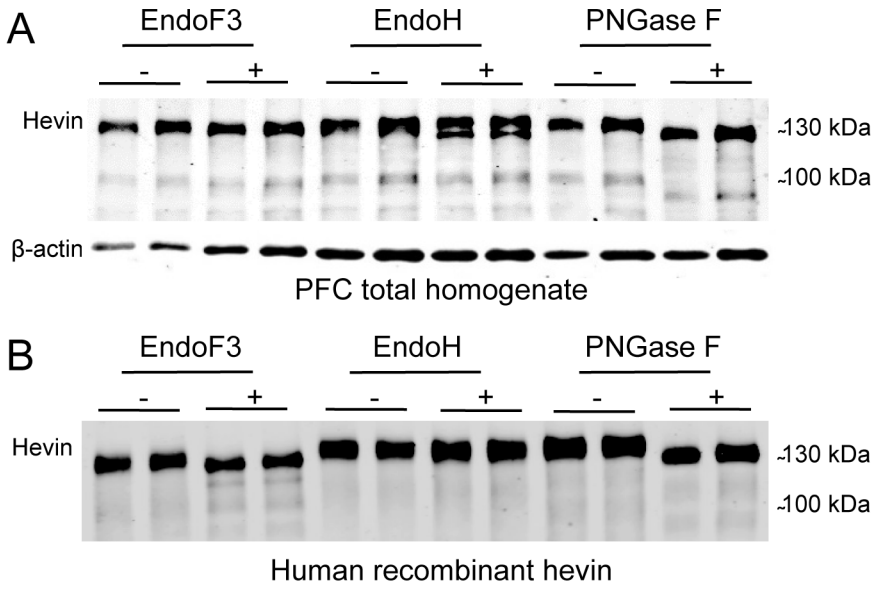

Figure 2. Distinct glycosylation patterns of hevin in human brain. A, B) Hevin immunoreactivity in a PFC total homogenate (A) and in human recombinant (B) hevin after treatment with EndoF3, EndoH or PNGaseF enzymes for 5 h at 37°C. Experiments were performed in triplicates. Representative western blot image for each experiment is shown.

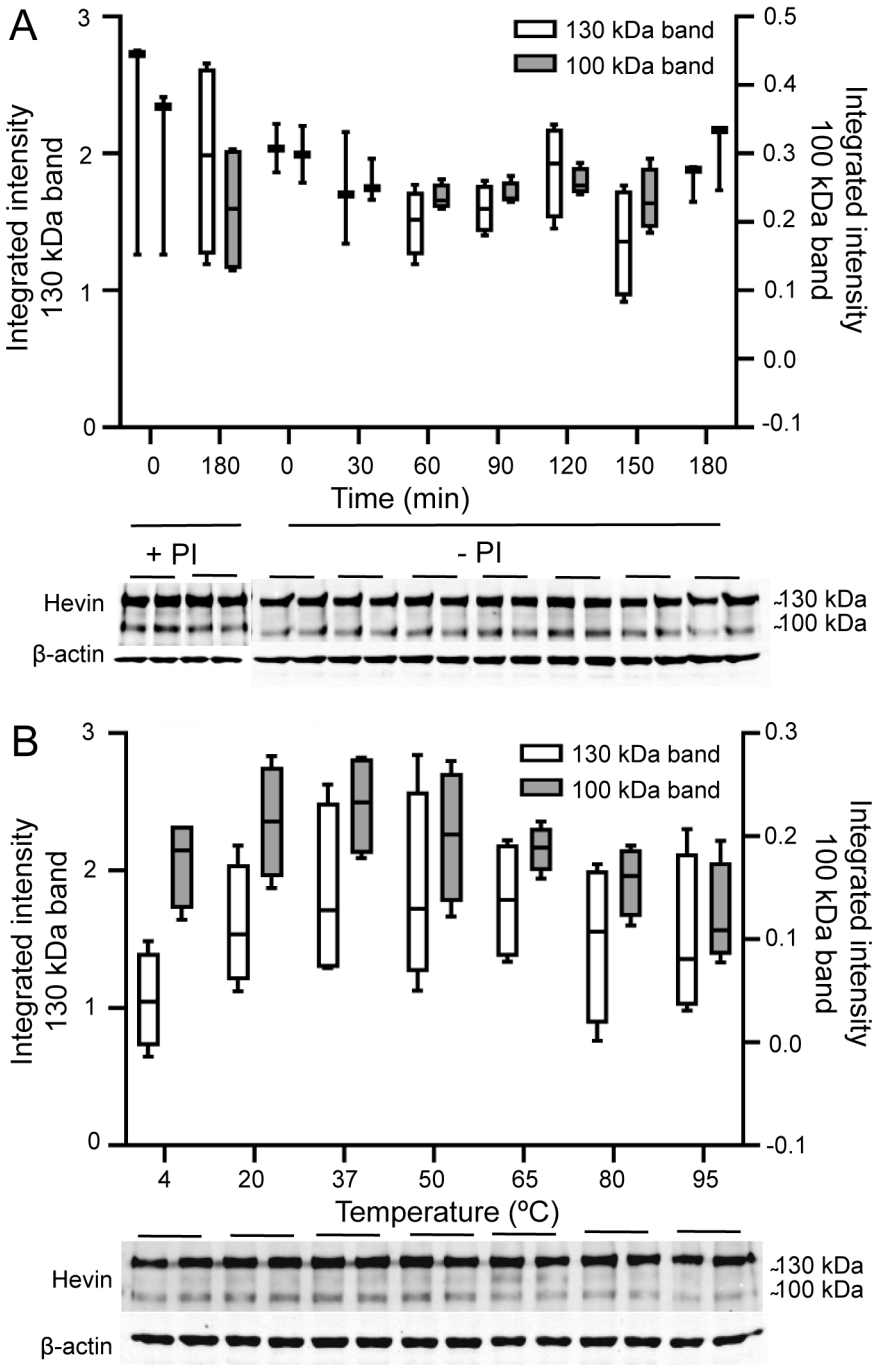

Figure 3. Proteolytic degradation of hevin in human brain. A) Hevin immunoreactivity and corresponding ß-actin-normalized quantification in a PFC total homogenate pool (20 µg) after incubation with (+PI) or without (-PI) protease inhibitors for a duration of 0 to 180 min at 37°C. B) Hevin immunoreactivity and corresponding ß-actin-normalized quantification in a PFC total homogenate pool (20 µg) after incubation at different temperatures (4°C–95°C) for 15 min. Experiments were performed in triplicates. Representative western blot image for each experiment is shown.

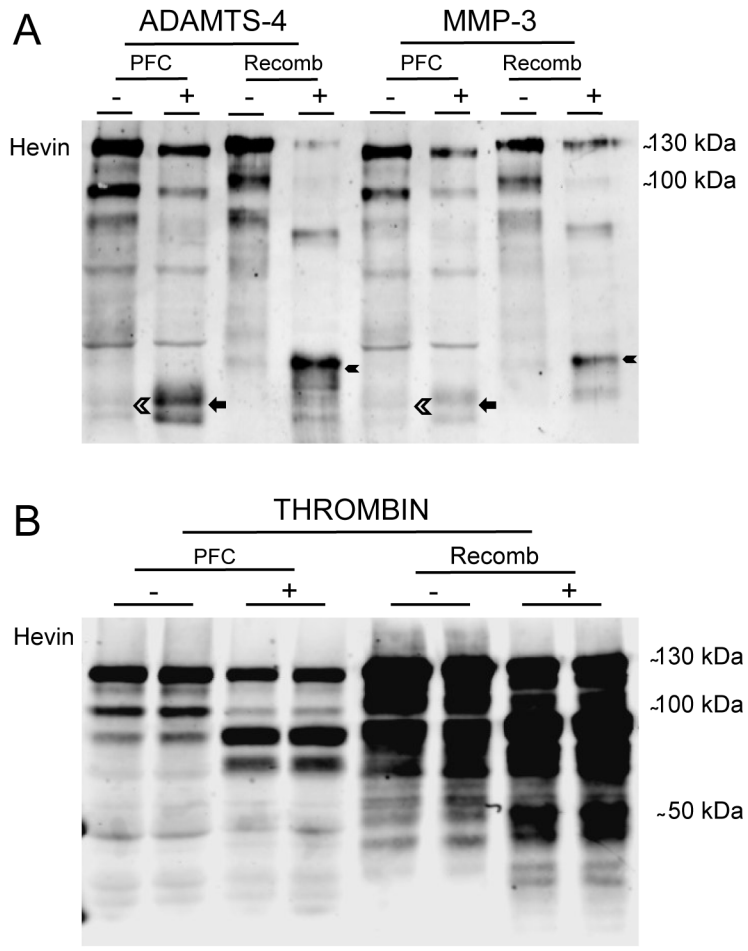

Figure 4. Sensitivity of human hevin to matrix metalloproteases and the serine protease thrombin. A) Hevin immunoreactivity in a PFC total homogenate and in human recombinant hevin after treatment with after treatment with ADAMTS4 or MMP-3 enzymes for 5 h at 37°C (*arrow*: ~40 kDa double band detected in digested-PFC; *filled arrowhead*: ~47 kDa double band detected in digested-recombinant protein; *empty arrowhead*: hypothetical ~40 kDa SLF fragment in non-digested PFC). B) Hevin immunoreactivity of PFC total homogenate pool (70 µg) or human recombinant hevin (20 ng) after 15h (37°C) of incubation in the presence or absence of thrombin (1 U). Experiments were performed in duplicate and a representative western blot image is shown.

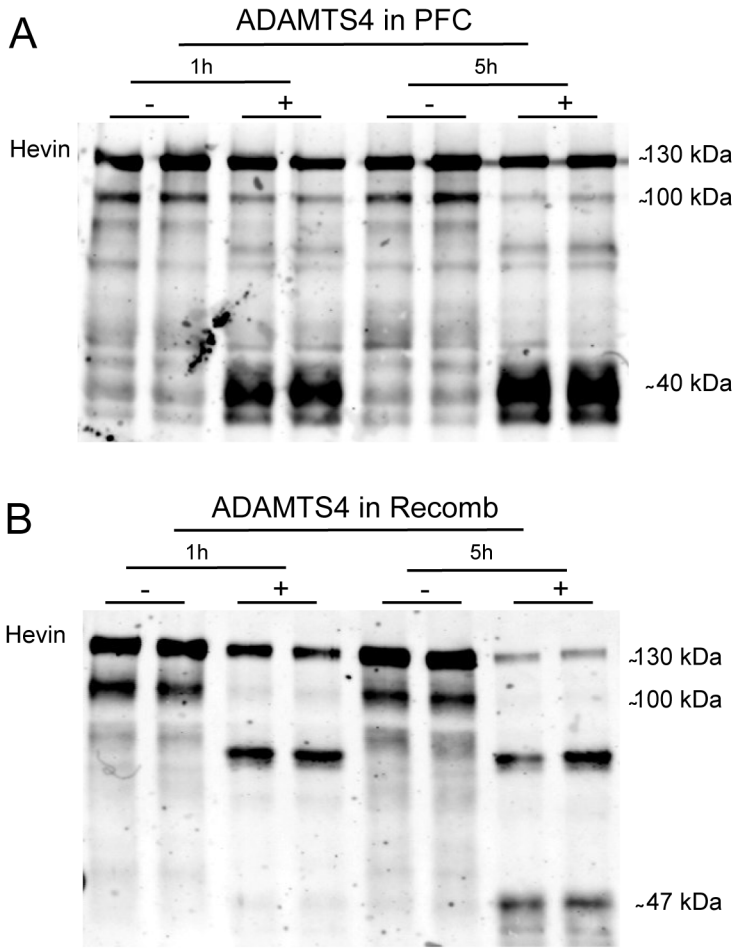

Figure 5. ADAMTS4-dependent proteolysis of human hevin. A) Hevin immunoreactivity of PFC total homogenate pool (50 µg), B) and human recombinant hevin (140 ng) after 1h or 5h (37°C) of incubation in the presence or absence of ADAMTS4 (2 µg) protease. Experiments were performed in duplicate and a representative western blot image is shown.

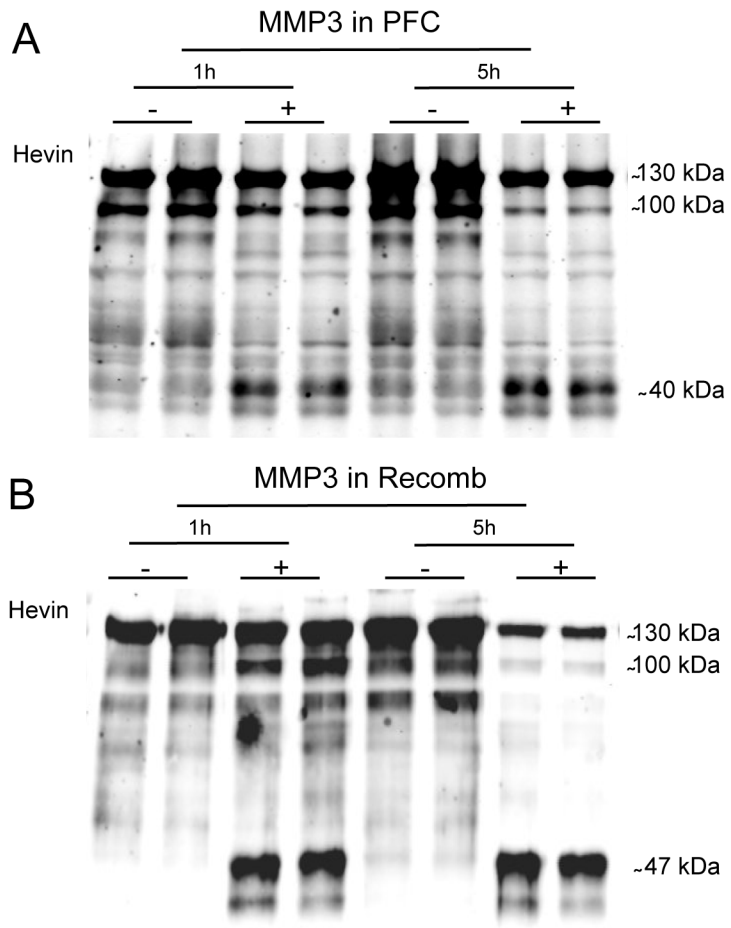

Figure 6. MMP3-dependent proteolysis of human hevin. A) Hevin immunoreactivity of PFC total homogenate pool (50 µg), B) and human recombinant hevin (140 ng) after 1h or 5h (37°C) of incubation in the presence or absence of MMP-3 protease (0.4 µg). Experiments were performed in duplicate and a representative western blot image is shown.

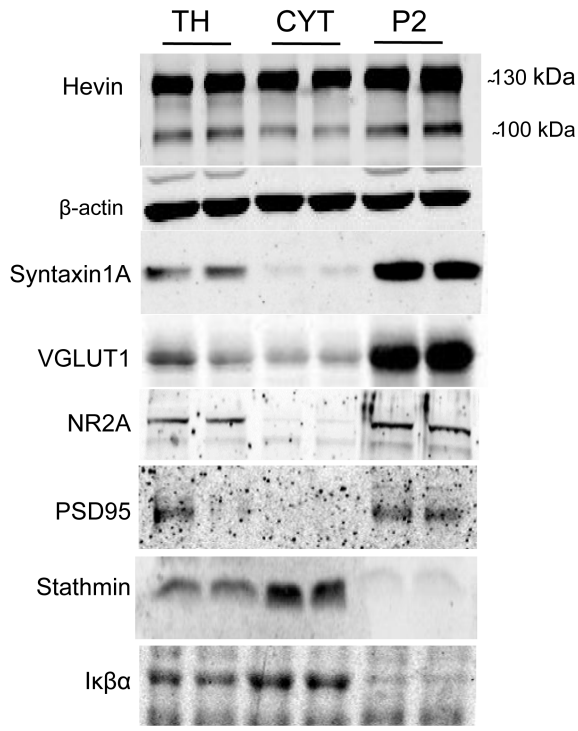

Figure 7. Human hevin expression in membrane-enriched and cytosolic fraction. Validation of the subcellular isolation of cytosol and P2 fractions from human PFC samples. Immunoreactivities of synaptic proteins (Syntaxin1A, VGLUT1, NR2A, PSD95) are enriched in P2 membrane fraction. Immunoreactivities of cytosolic proteins (Stathmin, IKβα) are enriched in cytosolic fraction. Western blot experiments were performed using a goat anti-human hevin antibody (R&D Systems, AF2728) and those specified in Table 1. Experiments were performed in duplicate and a representative western blot image is shown. *TH: total homogenate, CYT: cytosol, P2: membrane-enriched fraction.*

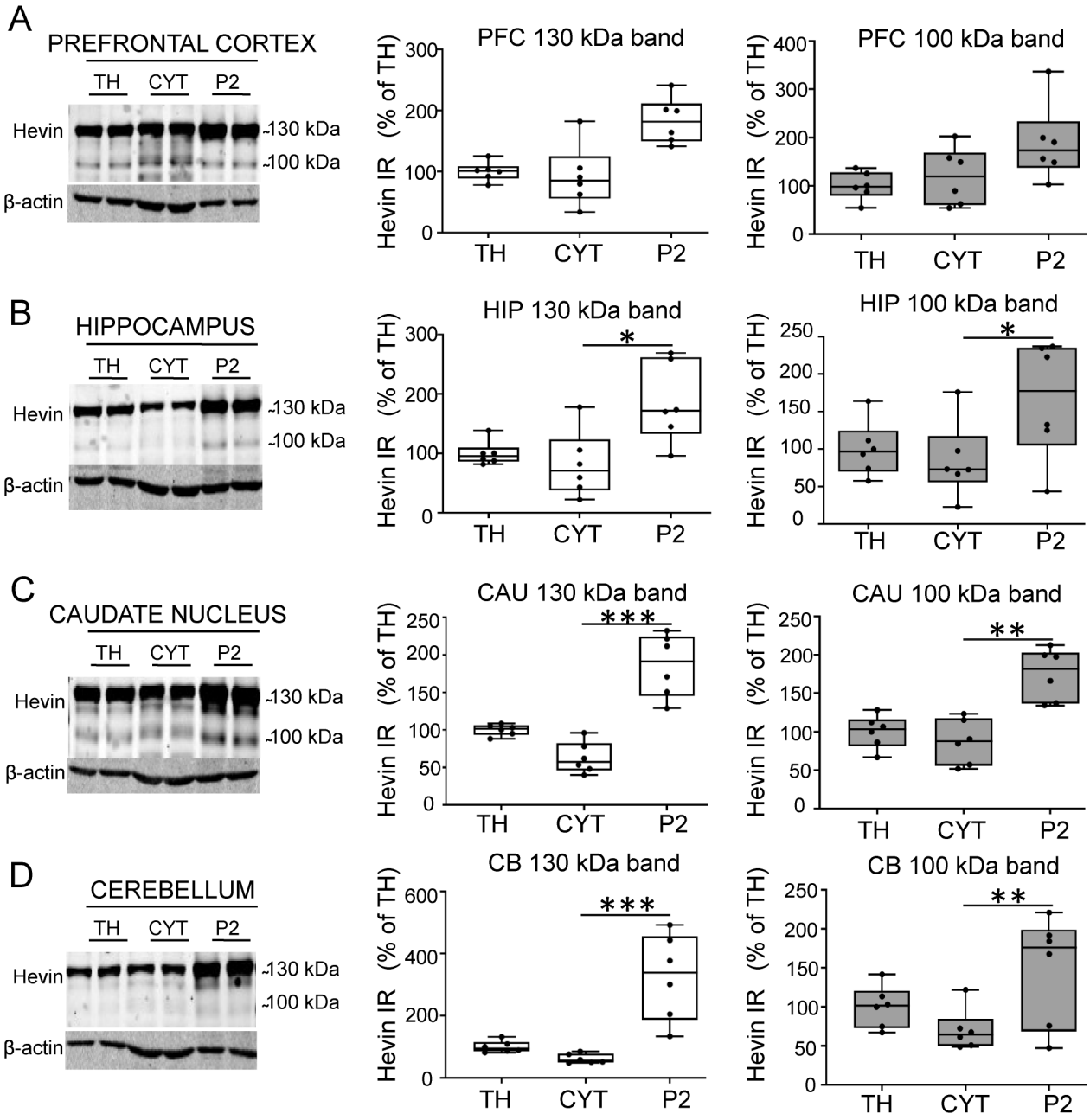

Figure 8. Prominent expression of hevin in membrane-enriched fraction along different brain regions. A-D) Hevin immunoreactivity and its ~130 kDa and ~100 kDa bands quantification (ß-actin-normalized) in different cellular preparations (*TH: total homogenate, CYT: cytosol, P2: membrane-enriched fraction*) obtained from prefrontal cortex (A), hippocampus (B), caudate nucleus (C) and cerebellum (D). Representative western blot images are shown in the figure. Kruskal-Wallis followed by Dunn's multiple comparisons test was used for each comparison. IR: immunoreactivity. PFC 130 kDa: $H_2 = 9.696$; CYT vs P2: $p = 0.004$; PFC 100 kDa: $H_2 = 5.626$; CYT vs P2: $p = 0.117$; HIP 130 kDa: $H_2 = 7.17$; CYT vs P2: $p = 0.011$; HIP 100 kDa: $H_2 = 4.363$; CYT vs P2: $p = 0.04$; CAU 130 kDa: $H_2 = 14.36$; CYT vs P2: $p = 0.0002$; CAU 100 kDa: $H_2 = 11.66$; CYT vs P2: $p = 0.0014$; CB 130 kDa: $H_2 = 14.75$; CYT vs P2: $p = 0.0001$; CB 100 kDa: $H_2 = 4.994$; CYT vs P2: $p = 0.0266$. Significance levels: *p< 0.05, **p< 0.01, ***p< 0.001, ****p< 0.0001. Brain regions were collected from 6 individuals. Experiments were performed in duplicate. Data points are added to the box-and-whiskers plot.

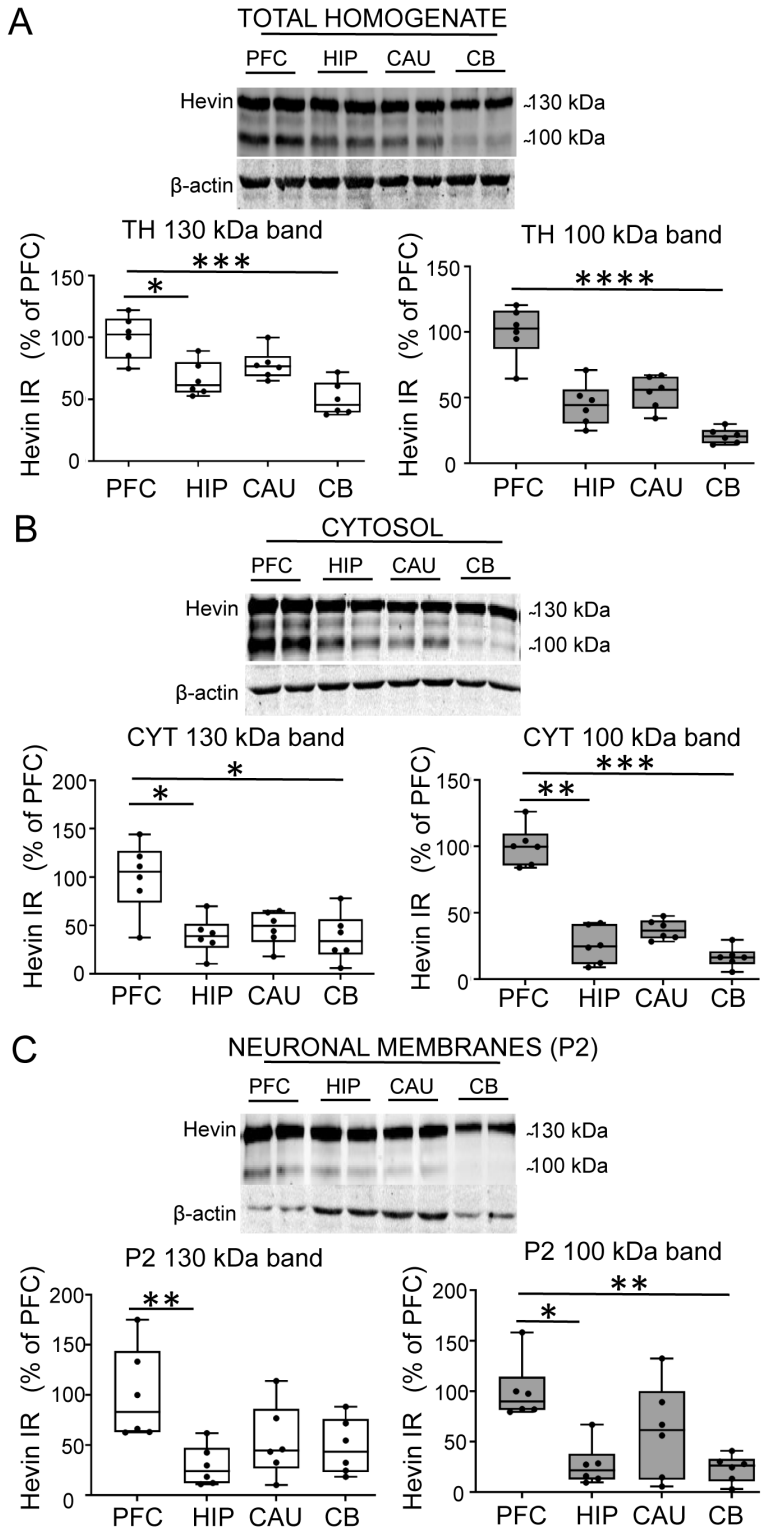

Figure 9. Comparison of human hevin expression among different brain regions. A-D) Hevin immunoreactivity and its ~130 kDa and ~100 kDa bands quantification (ß-actin-normalized) in different brain areas (PFC: prefrontal cortex, HIP: hippocampus, CAU: caudate nucleus, CB: cerebellum). Representative western blot images are shown in the figure. Kruskal-Wallis followed by Dunn's multiple comparisons test was used for each comparison. IR: immunoreactivity. TH 130 kDa: $H_3 = 15.02$; PFC vs HIP: $p = 0.043$; PFC vs CB: $p = 0.0006$; TH 100 kDa: $H_3 = 18.47$; PFC vs CB: $p = 0.0001$; CYT 130 kDa: $H_3 = 8.867$; PFC vs HIP: $p = 0.034$; PFC vs CB: $p = 0.027$; CYT 100 kDa: $H_3 = 17.21$; PFC vs HIP: $p = 0.006$; PFC vs CB: $p = 0.0003$; P2 130 kDa: $H_3 = 9.58$; PFC vs HIP: $p = 0.007$; P2 100 kDa: $H_3 = 11.49$; PFC vs HIP: $p = 0.013$; PFC vs CB: $p = 0.009$. Significance levels: *p< 0.05, **p< 0.01, ***p< 0.001, ****p< 0.0001. Brain regions were collected from 6 individuals. Experiments were performed in duplicate. Data points are added to the box-and-whiskers plot.

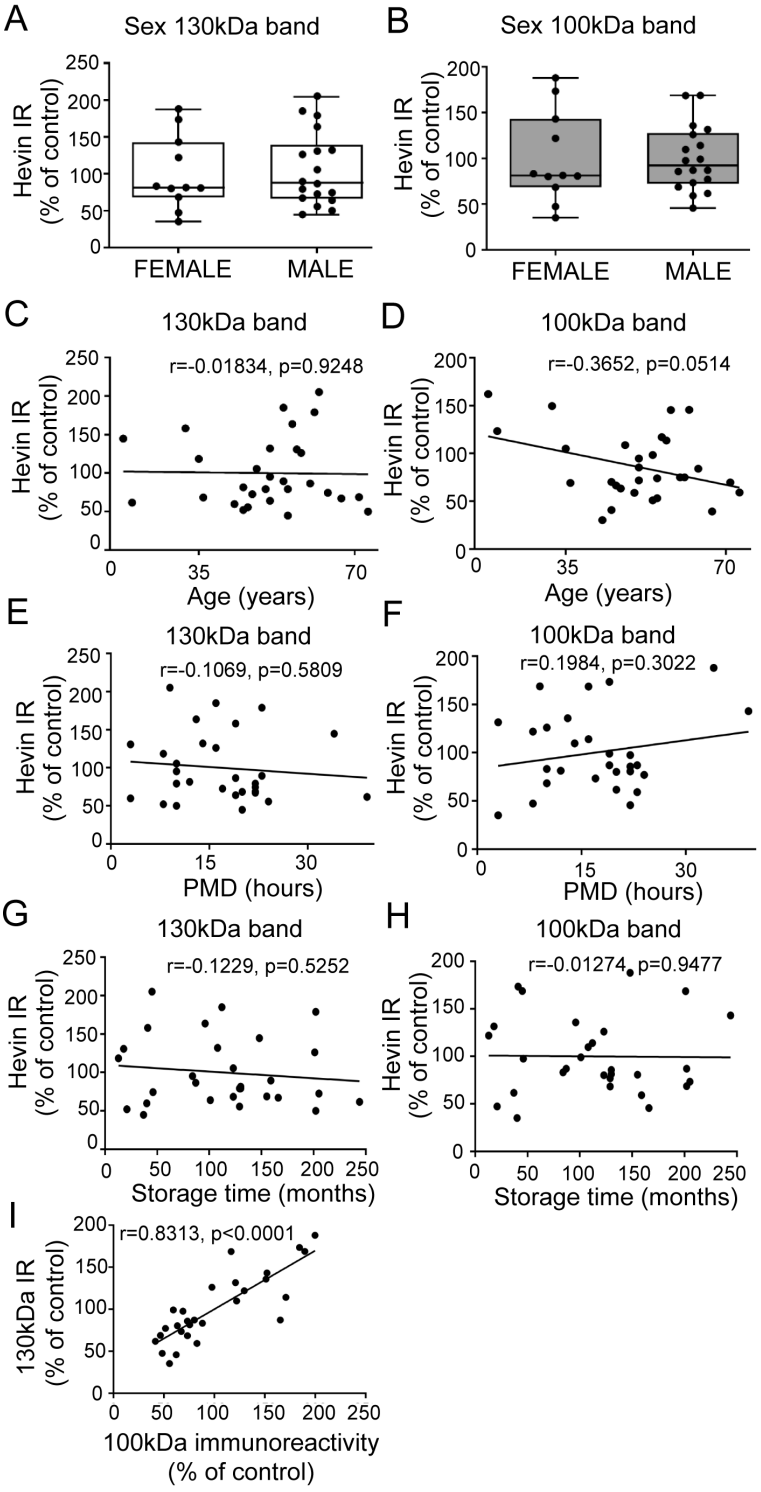

Figure 10. Influence of sex, age, PMD and storage time on hevin expression, and correlation between the two hevin isoforms. A-B) Sex comparison between 11 females and 18 males of ~130 kDa (A) and ~100 kDa (B) hevin bands immunoreactivity (ß-actin-normalized) in PFC total homogenates. Age (C-D), *postmortem* delay (E-F) and storage time (G-H) correlation with the immunoreactivity of the ~130 kDa and ~100 kDa bands in total homogenate preparations obtained from human PFC of 29 control subjects. I) Statistical linear correlation of hevin ~130 kDa and ~100 kDa bands immunoreactivities in PFC total homogenate pool of 29 subjects. IR: immunoreactivity. Statistical comparison between sexes was performed by two-tailed Student's t-test and correlation analyses by two-tailed Pearson´s correlation test. No statistically significant linear correlations were observed (Pearson' *r* value and p value are shown in each correlation graph). Simple linear regression analysis showed correlation between the levels of the 130 kDa band with the 100 kDa band ($r = 0.8313$, $p \leq 0.0001$). Prefrontal cortex samples of 29 subjects were used and run in triplicate.

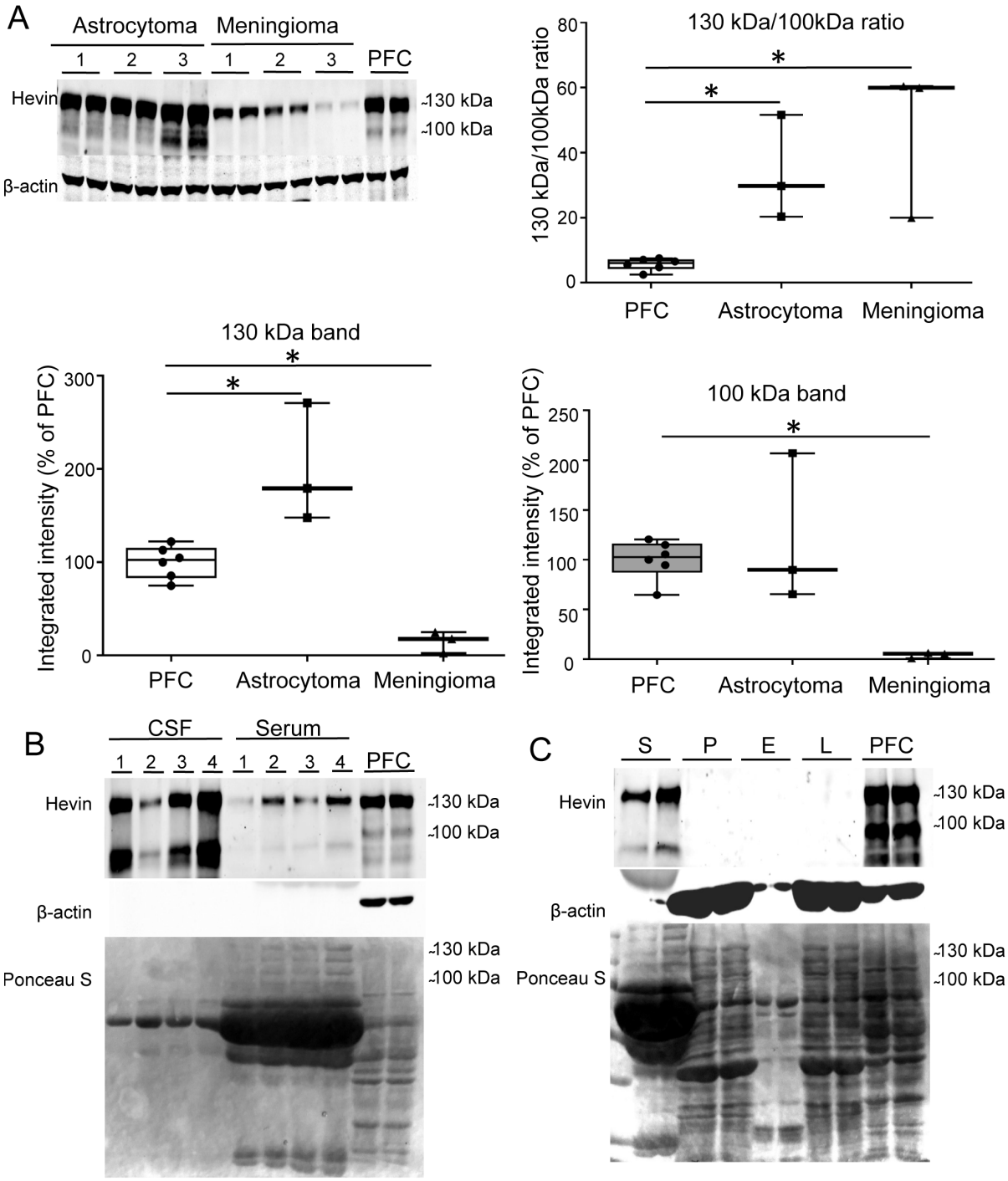

Figure 11. Strong expression of hevin in astrocytoma, meningioma and CSF but not in any blood cell type. A) Hevin immunoreactivity and corresponding ß-actin-normalized quantifications in total homogenate preparations of 3 astrocytoma (18 µg), 3 meningioma (18 µg) and 6 PFC samples (15 µg). B) Hevin immunoreactivity in 4 CSF (3.6 µg) and 4 serum samples (3.6 µg). C) Hevin immunoreactivity in different blood fractions (S: serum, P: platelets, E: erythrocytes, L: leucocytes). The same amount of protein was loaded for each sample (37 µg) with the exception of leucocytes (8 µg, due to the sample concentration). β-actin (only present in PFC and serum samples) and Ponceau S staining are also shown. Experiments were performed in duplicate. Representative western blot image is shown. The statistical comparison between astrocytoma, meningioma and PFC was done by Mann-Whitney test. 130 kDa, PFC vs Astrocytoma: $U_{6,\ 3} = 0.024$; 130 kDa, PFC vs Meningioma: $U_{6,\ 3} = 0.024$; 100 kDa, Astrocytoma vs Meningioma : $U_{3,\ 3} = 0.024$; 130 kDa / 100 kDa ratio, PFC vs Astrocytoma: $U_{6,\ 3} = 0.024$; Astrocytoma vs Meningioma : $U_{3,\ 3} = 0.024$. Samples were run in duplicate. Significance levels: *p< 0.05. Data points are added to the box-and-whiskers plot.